Synthesis of Diiron Bridging Allenylidene Complexes $Cp^*_2Fe_2(\mu\text{-}C{=}C{=}CR^1R^2)(\mu\text{-}CO)(CO)_2$ ($Cp^* = \eta^5\text{-}C_5Me_5$) via Nucleophilic Addition to the Diiron Ethynediyl Complex $(\mu\text{-}C{\equiv}C)[FeCp^*(CO)_2]_2$ and Their Conversion to Cationic μ-Vinylcarbyne and μ-Vinylidene Complexes

Munetaka Akita,* Shin-ichi Kato, Masako Terada, Yoshiko Masaki, Masako Tanaka, and Yoshihiko Moro-oka*

Research Laboratory of Resources Utilization, Tokyo Institute of Technology, 4259 Nagatsuta, Midori-ku, Yokohama 226, Japan

Received December 30, 1996[⊗]

A variety of diiron bridging allenylidene complexes, $Cp^*_2Fe_2(\mu\text{-}C{=}C{=}CR^1R^2)(\mu\text{-}CO)(CO)_2$ (**3**; R^1, R^2 = H, H (**a**); Me, Me (**b**); *n*-Bu, *n*-Bu (**c**); H, Ph (**d**); H, *t*-Bu (**e**); Me, Ph (**f**); Me, *n*-Bu (**g**); *t*-Bu, Me (**h**)) are prepared by (i) addition of an excess amount of nucleophile (RLi, $LiHBEt_3$) to the diiron μ-ethynediyl complex $(\mu\text{-}C{\equiv}C)[FeCp^*(CO)_2]_2$ (**1**) *in portions* (one-pot synthesis) or (ii) nucleophilic addition to the diiron μ-acylvinylidene complex $Cp^*_2Fe_2[\mu\text{-}C{=}C(H){-}C(=O)R^1](\mu\text{-}CO)(CO)_2$ (**2**), which is also obtained from **1** (two-step synthesis). On the other hand, addition of an excess amount of nucleophile *in one portion* produces diacyl−vinylidene complexes $Cp^*_2Fe_2[\mu\text{-}C{=}C\{C(=O){-}R\}_2](CO)_2(\mu\text{-}CO)$ (**4**). Hybridization of the $Fe_2[\mu\text{-}C{=}C{=}CR^1R^2]$ moiety in **3** is similar to that in organic allene molecules, as revealed by X-ray crystallographic and spectroscopic analysis. Formation of **3** instead of the μ-alkenylvinylidene complex **4** (when either of R^1 or R^2 bears an α-hydrogen atom) can be interpreted in terms of steric repulsion between the bridging ligand and the Cp* ligands. In addition, the C−C coupling observed during the formation of **3** also proceeds in mononuclear iron acetylide complexes, $(\eta^5\text{-}C_5R_5)Fe(CO)_2\text{-}C{\equiv}C\text{-}Ph$ (**12**) (R= H (**a**), Me (**b**)), upon treatment with nucleophiles (Nu) to give enone $PhCH{=}CHC(=O){-}Nu$ (**13**) and alkenyl complexes, $(\eta^5\text{-}C_5R_5)Fe(CO)(PPh_3){-}C[C(=O){-}Nu]{=}C(H)Ph$ (**15**) (in the presence of PPh_3). The μ-allenylidene complexes **3** turn out to be amphoteric. Protonation of **3** takes place at the β-carbon atom of the μ-allenylidene bridge to give cationic μ-vinylcarbyne species $Cp^*_2Fe_2[\mu\text{-}\{C{-}C(H){-}C\}^+R^1R^2](\mu\text{-}CO)(CO)_2$ (**11**; R^1, R^2 = H, H, (**a**); Me, Me (**b**); H, Ph (**c**)), which have been characterized by NMR ($\delta_C(C_\alpha) > 450$) and X-ray crystallography (**11c**·BF_4). Subsequent nucleophilic addition gives a variety of functionalized μ-vinylidene complexes $Cp^*_2Fe_2[\mu\text{-}C{=}C(H){-}CR^1R^2Nu](\mu\text{-}CO)(CO)_2$ (**18**) through addition to the γ-carbon atom. In contrast, nucleophilic addition to **3** takes place at the γ-carbon atom, and μ-vinylidene complex **18** (reaction with $LiHBEt_3$) or cyclic product **21** (reaction with *n*-BuLi) are obtained after protonolysis. Thus, it has been clarified that the electrophile and nucleophile attack the β- and γ-carbon atoms of the bridging allenylidene ligand, respectively. The configuration of the bridging ligand (X) and the Fe auxiliary ligands (Cp* and CO) in a series of diiron bridging hydrocarbyl complexes, $Cp^*_2Fe_2(\mu\text{-}X)(\mu\text{-}CO)(CO)_2$ (X = allenylidene, vinylidene, and alkylidene), is also discussed on the basis of the molecular structure of **3a**−**c**, **4**, **18e**,**h**,**k**, and a μ-alkylidene complex $Cp^*_2Fe_2[\mu\text{-}C(H)CH_2CH_3](\mu\text{-}CO)(CO)_2$ (**19a**), which are obtained in the present study. The dinuclear complexes relieve the steric repulsion among the X and Cp* ligands by a combination of a stretching and twisting of the X part and precession of the Cp* ligands.

Introduction

Allenylidene species $C{=}C{=}CR_2$ belong to the family of cumulenylidene species $[(C{=})_mCR_2]$, which have been stabilized by interaction with transition metal fragments.[1] In contrast to well-established transition metal vinylidene complexes ($M_n{=}C{=}CR_2$; m = 1), the structure and reactivity of their next higher homologues, i.e., transition metal allenylidene complexes ($M_n{=}C{=}C{=}CR_2$; m = 2), have remained far less developed (Chart 1). This is mainly due to their limited accessibility.

Dehydration of a γ-hydroxyvinylidene intermediate, which is formed by treatment of a metal complex with a propargyl alcohol derivative, is the only systematic preparative method for mononuclear allenylidene complexes.[2] Further interaction with a labile metal species

[⊗] Abstract published in *Advance ACS Abstracts,* May 1, 1997.

(1) Bruce, M. A. *Chem. Rev.* **1991**, *91*, 197.

(2) (a) Selegue, J. P. *Organometallics* **1982**, *1*, 217. (b) Werner, H.; Rappert, T. *Chem. Ber.* **1993**, *126*, 669. (c)Werner, H.; Rappert, T.; Wiedeman, R.; Wolf, J.; Mahr, N. *Organometallics* **1994**, *13*, 2721. (d) Touchard, D.; Pirio, N.; Dixneuf, P. H. *Organometallics* **1995**, *14*, 4920. (e) Touchard, D.; Pirio, N.; Toupet, L.; Fettouhi, M.; Ouahab, L.; Dixneuf, P. H. *Organometallics* **1995**, *14*, 5263. (f) Touchard, D.; Guesmi, S.; Bouchaib, M.; Haquette, P.; Daridor, A.; Dixneuf, P. H. *Organometallics* **1996**, *15*, 2579. For higher cumulenylidene complexes, see, for example: (g) Touchard, D.; Haquette, P.; Daridor, A.; Toupet, L.; Dixneuf, P. H. *J. Am. Chem. Soc.* **1994**, *116*, 11157.

S0276-7333(96)01104-1 CCC: $14.00

Chart 1

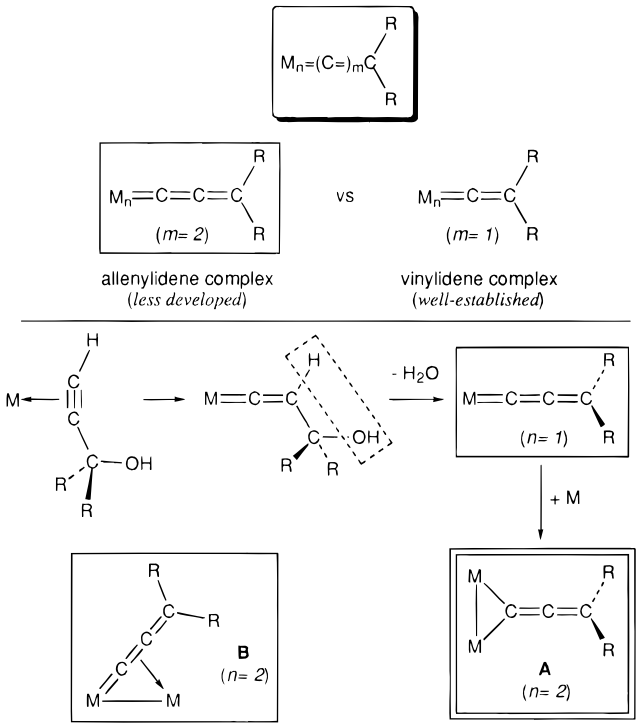

would lead to polynuclear complexes (Chart 1).[3c−e] However, such examples are very few, and no other rational synthetic method for dinuclear complexes is available until now. A limited number of previous studies have revealed two types of coordination modes: symmetrical μ-η^1:η^1 (**A**) and side-on μ-η^1:η^2 (**B**). The dicyano-substituted diiron complex $Cp_2Fe_2[\mu$-C═C═C(CN)$_2]$(μ-CO)L_2 (L_2 = dppm, dppe), reported by Etienne[3a] may be the most thoroughly studied example of an **A**-type complex, and it was prepared by a curious condensation reaction of a μ-vinylidene complex, $Cp_2Fe_2(\mu$-C═$CH_2)(\mu$-CO)L_2, and TCNE, accompanied by elimination of $CH_2(CN)_2$. On the other hand, **B**-type complexes have been found for group 6 metal complexes.[4] Let us point out that all of the previous examples except for **B**-type complexes contain substituents at the allenylidene terminus (C_γ), which may prevent decomposition through a C_γ attack, and that a parent allenylidene complex (M_n═C═C═CH_2) has never been reported so far.

Recently, we have been studying the chemical reactivity of the diiron μ-ethynediyl complex, Fp*−C≡C−Fp* (**1**; Fp* = $FeCp^*(CO)_2$).[5] In a previous paper, we reported a nucleophilic addition to **1** leading to a diiron bridging acyl−vinylidene complex, $Cp^*_2Fe_2[\mu$-C═C-(H)−C(═O)−R](μ-CO)$(CO)_2$ (**2**) via C−C coupling of the C_2 bridge, CO, and a nucleophile (Scheme 1).[5d,e] During the course of our study, we have found that addition of an excess amount of nucleophile furnishes different products, i.e., diiron bridging allenylidene complex $Cp^*_2Fe_2(\mu$-C═C═$CR^1R^2)(\mu$-CO)$(CO)_2$ (**3**) and diiron diacyl−vinylidene complex $Cp^*_2Fe_2[\mu$-C═C{C(═O)R}$_2$](μ-CO)-$(CO)_2$ (**4**), and that the selectivity of the reaction depends on *how the nucleophile is added*. Herein, we disclose the details of the nucleophilic addition reaction of **1**. We have established that the present method serves as a versatile synthetic method for type-**A** diiron bridging allenylidene complexes, $Cp^*_2Fe_2(\mu$-C═C═$CR^1R^2)(\mu$-CO)-$(CO)_2$ (**3**), and structural and reaction aspects of **3** will be also discussed.[6]

Scheme 1

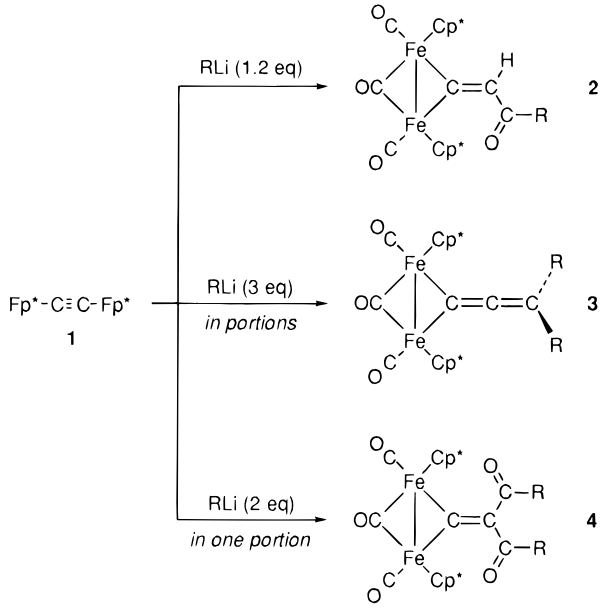

[Cp* = η^5-C_5Me_5; Fp* = $FeCp^*(CO)_2$]

Results and Discussion

Nucleophilic Addition to Ethynediyl Diiron Complex 1: One-Pot Synthesis of the Diiron Bridging Allenylidene Complexes 3. Addition of a slightly excess amount of nucleophile (RLi, $LiHBEt_3$) to **1** produced the bridging acyl-substituted vinylidene complex $Cp^*_2Fe_2[\mu$-C═C(H)−C(═O)−R](μ-CO)$(CO)_2$ (**2**) after protonolysis, as reported previously.[5c,7] However, addition of an excess amount of nucleophile *in portions* gave rise to another product, **3** (eq 1).[6] TLC (thin layer chromatography) analysis of a reaction mixture after addition of a stoichiometric amount of nucleophile

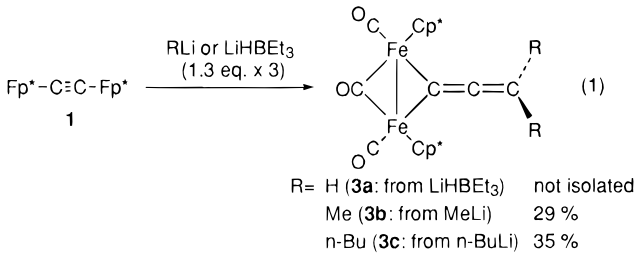

(3) (a) Etienne, M.; Talarmin, J.; Toupet, L. *Organometllics* **1992**, *11*, 2058. (b) Berke, H. *J. Organomet. Chem.* **1980**, *185*, 75. (c) Kolobova, N. E.; Ivanov, L. L.; Zhvanko, O. S.; Aleksandrov, G. G.; Struchkov, Y. T. *J. Organomet. Chem.* **1982**, *228*, 265. (d) Berke, H.; Härter, P.; Huttner, G.; Zsolnai, L. *Chem. Ber.* **1982**, *115*, 695. (e) Berke, H.; Härter, P.; Huttner, G.; Zsolnai, L. *Chem. Ber.* **1984**, *117*, 3432.

(4) (a) Froom, S. F. T.; Green, M.; Nagel, K. R.; Williams, D. J. *J. Chem. Soc., Chem. Commun.* **1987**, 1305. (b) Froom, S. F. T.; Green, M.; Mercer, R. J.; Nagel, K. R.; Orpen, A. G.; Rodrugues, R. A. *J. Chem. Soc., Dalton Trans.* **1991**, 3171. (c) Capon, J. F.; Le Berre-Cosquer, N.; Bernier, S.; Pichon, R.; Kergoat, R.; L'Haridon, P. *J. Organomet. Chem.* **1995**, *487*, 201.

(5) (a) Akita, M.; Moro-oka, Y. *Bull. Chem. Soc. Jpn.* **1995**, *68*, 420. (b) Akita, M.; Terada, M.; Oyama, S.; Moro-oka, Y. *Organometallics* **1990**, *9*, 816. (c) Akita, M.; Terada, M.; Oyama, S.; Sugimoto, S.; Moro-oka, Y. *Organometallics* **1991**, *10*, 1561. (d) Akita, M.; Terada, M.; Moro-oka, Y. *Organometallics* **1991**, *10*, 2961. The reaction mechanism has been corrected in ref 5e. (e) Akita, M.; Takabuchi, A.; Terada, M.; Ishii, N.; Tanaka, M.; Moro-oka, Y. *Organometallics* **1994**, *13*, 2516.

indicated formation of the acyl−vinylidene complex **2**.[5d,e] Further addition of nucleophile caused replacement of the spot of **2** by a new deep purple-red spot of **3**. Methanolysis followed by chromatographic separation led to isolation of the bridging allenylidene complex **3** in moderate yields. Because addition of the nucleophile *in one portion* led to the formation of another product (see below), it is crucial to add the nucleophile *in portions*. In addition, the amount of nucleophile should be adjusted carefully while checking the reaction by TLC, since addition of a too much of the nucleophile caused deterioration of **3**. Although the parent allenylidene complex **3a** could be formed by this method, it decomposed during chromatographic separation, and yet it could be isolated by the method mentioned below.

Reaction of Acyl−Vinylidene Complexes 2 with Nucleophiles: Two-Step Synthesis of 3. The detection of the acyl−vinylidene complex **2** suggested that **2** or its derivative was an intermediate of **3**. As was anticipated, treatment of an isolated sample of **2** with a slightly excess amount of nucleophile led to the formation of **3** (eq 2). The reaction was much cleaner

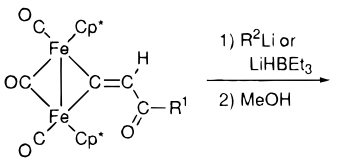

2

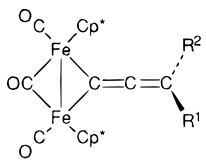

3

	R^1	R^2	Yield
3a	H	H	53 %
3d	H	Ph	39 %
3e	H	Bu^t	22 %
3f	Me	Ph	78 %
3g	Me	Bu^n	38 %
3h	Bu^t	Me	55 %

(2)

than the above-mentioned one-pot synthesis, and therefore, the product could be isolated by simple filtration through an alumina plug followed by crystallization. The parent allenylidene complex **3a** could be isolated in 53% yield by this method.

By changing the two nucleophiles (R^1 and R^2) added, unsymmetrically substituted bridging allenylidene complexes **3d**−**h** were also prepared successfully. To the best of our knowledge, monosubstituted allenylidene complexes [M_n{=C=C=C(H)R}] like **3d**,**e** are unprecedented, except for **B**-type complexes, and **3a** is the first example of a parent allenylidene complex [M_n-(=C=C=CH_2)]. Most of previous examples contain bulky (e.g., *t*-Bu) or unsaturated substituents (e.g., Ph, CN), so as to prevent attack at the allenylidene terminus (C_γ). The steric shielding of the allenylidene group by the Cp* ligands may lead to successful isolation of **3**, as will be discussed later.

The reaction of **2** with an organolithium reagent without an α-hydrogen atom (e.g., *t*-BuLi, PhLi) was very clean. However, it is notable that reaction with an alkyllithium bearing an α-hydrogen atom produced the alkenyl vinylidene complex **5** (eq 3).[8,9] In particular,

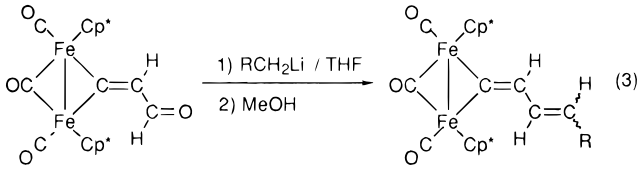

2a

R= H (**5a**) 76 %
n-Pr (**5b**) 67 %

(3)

5 was formed exclusively from the aldehyde complex **2a**.

Characterization of the Diiron Bridging Allenylidene Complexes 3. The bridging allenylidene complexes **3** are readily characterized on the basis of their spectroscopic data, in particular the ^{13}C-NMR data (Table 1), though they show spectroscopic features very similar to those of related bridging vinylidene complexes $Cp^*_2Fe_2(\mu\text{-}C{=}CR_2)(\mu\text{-}CO)(CO)_2$ (see below). The presence of the three allenylidene carbon atoms is indicated by the ^{13}C-NMR resonances appearing in the range of 77−210 ppm. The most shielded signal observed around 77−114 ppm is assigned unequivocally to C_γ on the basis of the signals of **3a**,**d**,**e** with $^1J_{CH}$ coupling. As for the remaining two quaternary carbon signals, the lowest and the middle signals have been assigned tentatively to C_β and C_α, respectively, because $^2J_{CH}$ coupling is observed for C_β in **3d**,**e**. The α-carbon signal is observed in a considerably shielded region compared to that of the μ-vinylidene complex (cf. **18**, δ_C 280−290; see below), and the δ_C values for the β- and γ-carbon atoms are comparable to those for allene [CH_2=C=CH_2, $\delta_C(CH_2)$ 74.8; δ_C(=C=) 213.5].[10] A similar ^{13}C-NMR pattern has been observed for the previously reported **A**-type complexes, except for the Mn_2 and MnFe complexes.[3] The simple NMR pattern for the $Cp^*_2Fe_2(\mu\text{-}CO)(CO)_2$ auxiliary of the symmetrical derivatives **3a**−**c** with single Cp* and CO resonances suggests a C_2-symmetrical structure, which has been confirmed by X-ray crystallography.[11]

The molecular structure of the symmetrical allenylidene complexes **3a**,**b**, **3c′** (the η^5-C_5Me_4Et derivative of **3c**) has been determined by X-ray crystallography. ORTEP views and a space-filling model are shown in Figures 1−4 and structural parameters are given in Table 2. At first, the allenylidene moiety (C1−C2−C3) is essentially linear and the CR_2 plane is laid almost perpendicular to the Fe1−Fe2−C1 triangle. The similar C1−C2 and C2−C3 distances fall in the typical range of C(sp^2)=C(sp) bond lengths (1.31 Å),[12] though the former is slightly longer than the latter. These struc-

(6) A preliminary report has appeared. Terada, M.; Masaki, Y.; Tanaka, M.; Akita, M.; Moro-oka, Y. *J. Chem. Soc., Chem. Commun.* **1995**, 1611.

(7) Reaction of **1** with PhLi resulted in replacement of the ethynyl moiety to give Fp*−Ph.

(8) (a) Casey, C. P.; Marder, S. R. *Organometallics* **1985**, *4*, 411. (b) Casey, C. P.; Konings, M. S.; Palermo, R. E.; Colborn, R. E. *J. Am. Chem. Soc.* **1985**, *107*, 5296. (c) Casey, C. P.; Konings, M. S.; Marder, S. R. *J. Organomet. Chem.* **1988**, *345*, 125.

(9) Although X-ray crystallography of **5a** was attempted, a centric space group indicated a completely disordered structure with respect to the midpoint of the Fe−Fe bond and the structure could not be refined satisfactorily. The CPK model (Figure 4) is based on a structure revealed by difference Fourier synthesis. Crystallographic data for **5a**: a = 18.609(7) Å, b = 8.888(2) Å, c = 17.905(6) Å, β = 121.15(2)°, V = 2534(2) Å^3, crystal system monoclinic, space group $C2/c$.

(10) Clerc, P.; Simon, S. *Tabellen zur Strukturaufklälung organischer Verbindungen mit spektroskopischen Methoden*; Springer: Berlin, 1981.

(11) No cumulene type C=C stretching vibration was observed for **3**, though such a vibration was reported for the CN-substituted deivative.[3a]

(12) March, J. *Advanced Organic Chemistry*; John Wiley & Sons: New York, 1985.

Published on May 27, 1997 on http://pubs.acs.org | doi: 10.1021/om961104e

Table 1. NMR and IR Data for Diiron Bridging Allenylidene Complexes, $Cp^*_2Fe_2(\mu\text{-}C_\alpha{=}C_\beta{=}C_\gamma R^1R^2)(\mu\text{-}CO)(CO)_2$ (3), and Diiron Bridging Vinylidene Complexes, $Cp^*_2Fe_2(\mu\text{-}C_\alpha{=}C_\beta(H_\beta){-}CR^1R^2{-}Nu)(\mu\text{-}CO)(CO)_2$ (18)[a]

complex (R^1, R^2, Nu)	^{1}H-NMR		^{13}C-NMR							IR
	R^1, R^2, (H_β, Nu)	Cp*	C_α	C_β	C_γ	R^1, R^2, (Nu)	C_5Me_5	C_5Me_5[b]	CO	ν(CO)
3a[c] (H, H, -)	5.47	1.59	202.3	206.5	77.6 (t, 167)		97.9	9.1	214.7, 276.4	1928, 1767
3b[d] (Me, Me, -)	2.00	1.62	191.9	206.4	100.9	26.1 (q, 122)	97.7	9.3	214.2, 280.5	1915, 1758
3c[d] (*n*-Bu, *n*-Bu, -)	0.94 (3H, t, 7.2),[e] 1.44 (4H, m),[f] 2.33 (2H, t, 7.0)[g]	1.62	191.5	206.1	111.4	14.1 (q, 123),[e] 22.9 (t, 124),[f] 31.3 (t, 124),[f] 37.7 (t, 127)[g]	97.8	8.8	214.0, 280.1	1920, 1771
3d[c] (H, Ph, -)	6.85 (1H, s),[h] 7.09−7.90 (5H, m)[i]	1.59, 1.60	193.8	200.6 (d, 10)	97.3 (d, 161)	125.4 (dt, 156, 7),[i,j] 126.8 (dt, 161, 7),[i,k] 129.1 (dd, 158, 9),[i,l] 143.1 (t, 7)[i,m]	98.1	8.6, 9.2	214.4, 214.7, 276.1	1925, 1774
3e[d] (H, *t*-Bu, -)	5.76 (1H, s),[h] 1.30 (9H, s)[i]	1.62, 1.68	192.3	210.0	109.4 (d, 163)	30.7 (q, 129),[i] 35.4[i]	97.5, 97.7	8.4, 9.1	213.7, 213.8, 291.6	1917, 1779
3f[c] (Me, Ph, -)	2.43,[h] 7.13−7.99[i]	1.56, 1.62	192.5	197.6	103.3	22.5 (q, 127),[h] 125.6 (dt, 164, 7),[i,j] 126.5 (dt (164, 7),[i,k] 127.4 (dt, 164, 7),[i,k] 128.5 (dd, 165, 7),[i,l] 129.0 (dd, 160, 7),[i,l] 145.0[i,m]	98.3, 98.7	8.9, 9.1	214.4, 214.6, 277.3	1918, 1773
3g[c] (Me, *n*-Bu, -)	1.02 (3H, t, 7.3),[e] 1.41 (2H, m),[i,f] 1.81 (2H, m),[i,f] 2.10 (3H, s),[h] 2.40 (2H, t, 7.0)[i,g]	1.62, 1.63	192.4	206.2	105.2	14.3 (q, 125),[i,e] 22.1 (q, 125),[h] 23.3 (t, 126),[i,f] 31.4 (t, 127),[i,f] 40.0 (t, 127),[i,g]	98.0, 98.6	8.9, 9.2	214.8, 214.9, 278.9	1920, 1773
3h[c] (*t*-Bu, Me, -)	1.48 (9H, s),[h] 2.07 (3H, s)[i]	1.60, 1.65	191.4	205.1	114.6	22.3 (q, 127),[i] 30.3 (q, 125),[h] 37.5[h]	97.8, 97.9	8.9, 9.2	214.1, 214.4, 279.2	1916, 1774
18a[d] (H, H, H)	2.52 (3H, d, 6.9),[h,i,o] 7.09 (1H, q, 6.9)[n]	1.60, 1.68	288.5	126.5 (dq, 151, 7)		21.4 (q, 127)	98.2, 98.3	8.9, 9.8	214.7, 214.8, 278.6	1924, 1774, 1602[p]
18b[d] (H, H, Me)	1.28 (3H, t, 7.3),[o] 2.89, 3.03 (1H × 2, m),[h,i] 6.99 (1H, dd, 4.9, 8.5)[n]	1.61, 1.67	286.5	135.5 (d, 155)		16.5 (q, 125),[o] 28.6 (t, 127)	98.0, 98.3	8.9, 9.8	214.6, 214.7, 278.5	1919, 1774
18c[c] (H, H, *n*-Bu)	1.05 (3H, t, 7.3),[o] 1.57, 1.59, 1.91, 3.12 (2H × 4, m),[h,i,o] 7.27 (1H, dd, 5.7, 7.6)[n]	1.58, 1.65	287.3	133.8		14.5 (q, 127),[o] 23.3, 32.4, 32.7, 36.2 (t × 4, 127)[h,i,o]	98.1, 98.4	9.0, 9.9	215.3, 215.5, 277.1	1914, 1778
18d[c,q] (H, H, Ph)	4.35 (1H, dd, 8.5, 14.1),[h,i] 4.52 (1H, dd, 4.9, 14.1),[h,i] 7.20−7.38 (4H, m),[o,r] 7.61 (2H, d, 7.6)[o]	1.45, 1.64								1918, 1778
18e[d] (Me, Me, H)	1.26 (3H, d, 6.7),[h,i] 1.36 (3H, d, 6.5),[h,i] 3.26 (1H, m),[o] 6.88 (1H, d, 8.8)[n]	1.62, 1.68	283.5	141.7 (d, 155)		25.0, 26.4 (q, 127),[h,i] 32.5 (d, 127)	97.9, 98.3	8.9, 9.8	214.6, 214.7, 278.2	1917, 1771
18f[c] (Me, Me, Me)	1.66 (9H),[h,i,o] 7.46 (1H)[n]	1.55, 1.63	284.9	145.6 (d, 149)		36.2, 32.4 (q, 125)[h,i,o]	98.6, 98.9	9.0, 10.1	215.8, 216.5, 277.4	1924, 1769, 1574[p]
18g[c] (Me, Me, *n*-Bu)	1.07 (3H, t, 7.3),[o] 1.60, 1.66 (3H × 2),[h,i] 1.51, 1.87, 2.28 (2H × 3, m),[o] 7.51 (1H)[n]	1.57, 1.64	284.6	146.0 (d, 151)		14.7 (q, 125),[o] 29.0, 29.6 (q × 2, 125),[h,i] 38.8, 24.4, 27.5, 44.2 (t × 3, 125)	98.6, 98.9	9.0, 10.1	215.7, 216.4, 277.4	1923, 1774, 1571[p]
18h[d] (Me, Me, Ph)	7.85 (2H, d, 7.2),[l,o] 7.77 (1H),[n] 7.34 (2H, dd, 7.2, 7.6),[k,o] 7.18 (1H, t, 7.6),[j,o] 1.59, 1.95 (3H × 2)[h,i]	1.43, 1.65	283.8	143.8 (d, 150)		26.8, 38.6 (q × 2, 129),[h,i] 43.0, 125.1 (dt, 156, 6),[j,o] 126.6 (155, 6),[k,l,o] 153.5[m,o]	98.5, 99.0	8.9, 9.4	215.2, 216.0, 278.9	1915, 1772
18i[d] (H, Ph, Ph)	5.60 (1H, d, 9.8),[s] 7.05−7.10 (2H, m),[o] 7.36 (4H, t, 6.3),[o] 7.50 (1H, d, 9.8),[n] 7.69 (4H, d, 6.8)[o]	1.39, 1.61	284.2	135.8 (dd, 146, 6)		56.0 (d, 127),[s] 125.2 (dt, 162, 6),[j] 125.7 (dt, 162, 6)[j] 128.0 (dd, 159, 6),[l] 128.4 (dd, 159, 6),[l] 128.6 (dt, 146, 6),[k] 128.8 (dt, 146, 6),[k] 146.8 (d, 6), 149.2 (d, 6)[m]	98.5, 98.7	8.5, 9.1	214.6, 214.7, 277.4	1916, 1779
18j[c] (H, H, NEt_2)	1.28 (6H, t, 7.1),[o] 2.92 (4H, q, 7.2),[o] 4.02 (1H, dd, 8.2, 13.1),[h,i] 4.19 (1H, dd, 4.5, 13.1),[h,i] 7.46 (1H, dd, 4.7, 8.2)[n]	1.60, 1.65	288.7	131.1 (d, 151)		12.8 (q, 127),[o] 47.4 (t, 127),[o] 58.1 (t, 127)	98.4, 98.6	9.0, 9.9	215.2, 215.3, 276.9	1913, 1785, 1601[p]
18k (Cp*)	1.04, 1.74, 1.81, 1.90, 1.94 (3H × 5), 3.04 (1H, dd, 8.1, 14.6), 3.18 (1H, dd, 2.8, 14.6) 6.13 (1H, dd, 3.0, 8.3)[n]	1.49, 1.69	286.5	128.4 (dt, 154, 5)		22.3, 11.4, 11.1, 10.2, 10.0 (q × 5, 127), 56.7 (s), 40.7 (t, 125), 133.5, 134.0, 141.0, 142.0	98.0, 98.2	8.5, 9.9	214.4, 214.5, 278.4	1920, 1770, 1594[p]

[a] Observed at 400 (^{1}H) and 100 MHz (^{13}C). Chemical shifts are reported in ppm downfield from TMS. Multiplicity and coupling constants (Hertz; J_{HH} or J_{CH} unless otherwise stated) are shown in parentheses. The signals without a sign of multiplicity are singlets. IR spectra were recorded as KBr pellets. [b] Quartet signals (J_{CH} = 126−130 Hz). [c] NMR spectra were measured in benzene-d_6. [d] NMR spectra were measured in chloroform-*d*. [e] $CH_2(CH_2)_2CH_3$. [f] $CH_2(CH_2)_2CH_3$. [g] $CH_2(CH_2)_2CH_3$. [h] For R^1. [i] For R^2. [j] Para carbon atom signal of the Ph group. [k] Meta carbon atom signal of the Ph group. [l] Ortho carbon atom signal of the Ph group. [m] Ipso carbon atom signal of the Ph group. [n] H_β. [o] For Nu. [p] ν(C═C). [q] A pure sample was not obtained (see text). [r] H_β signal is overlapped with the Ph signals. [s] $C_\gamma H_\gamma$.

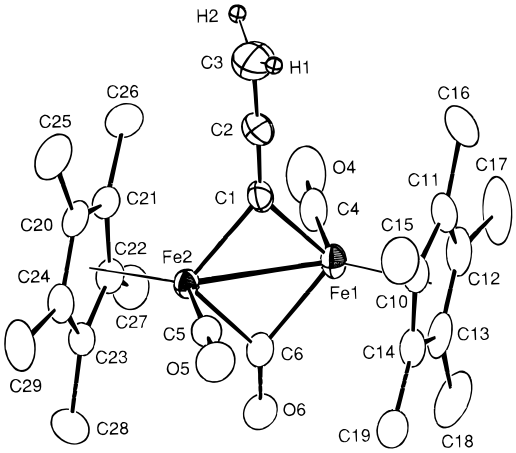

Figure 1. Molecular structure of **3a** drawn at the 30% probability level.

tural features indicate that the geometry of the $Fe_2[\mu$-$C{=}C{=}CR_2]$ moiety in **3** is essentially the same as that of organic allene molecules. As anticipated from the spectroscopic analysis, the molecules have a symmetrical structure with respect to the apparent C_2 axis passing through the allenylidene rod. As for the steric shielding by the Cp* rings, the β-carbon atom (C2) is surrounded by them to a considerable extent, as can be seen from the CPK model of **3b** (Figure 4). In addition, no apparent distortion is observed for the allene-like $R_2C{=}C{=}CFe_2$ moiety, as is evident from a top view (Figure 2b) and a CPK model of **3b** (Figure 4). The two methyl groups attached to the γ-carbon atom are tilted very slightly toward the Cp* rings. This means that no significant steric repulsion is present between the CR_2 moiety and the Cp* rings.

Formation Mechanism of 3. A plausible formation mechanism of **3** is summarized in Scheme 2. Initial nucleophilic attack at a Fe−CO group gives the anionic acyl intermediate **6**, which is converted to the η^2-alkyne complex-type intermediate $[Cp^*Fe(CO)\{\eta^2\text{-}Fp^*{-}C{\equiv}C{-}C(=O){-}R\}]^-$ via reductive elimination (from **6**) or migratory insertion of the acetylide group to the oxycarbene ligand (from **6′**). Subsequent slippage of the π-coordinated Fe moiety toward the other Fe center σ-bonded to the acetylide gives rise to the enolate intermediate **7**. Protonation of **7** furnishes the acyl−vinylidene complex **2**, as reported previously.[5d,e]

Further addition of the nucleophile to **7** results in the formation the dianionic alkoxide intermediate **8**, which is converted to the final product **3** via protonation (**9**) followed by dehydration. The nucleophilic addition to the anionic part in **7** may be sluggish because of its anionic nature. In the two-step synthesis, the reaction should proceed via the monoanionic alkoxide intermediate **10** analogous to **8**.

Let us discuss the dehydration step in detail. First of all, from a reaction mixture of **2a** and *t*-BuLi, a minor product assignable to the diprotonated form (**9a**) of **8** was isolated and characterized on the basis of its ^{1}H-NMR data (in $CDCl_3$) as well as a ν(OH) absorption (KBr) (Chart 2). The mechanism of the subsequent dehydration may resemble the acid-catalyzed dehydration of allylic alcohol (Scheme 3). Protonation of allylic alcohol followed by elimination of water gives allyl cation. Subsequent deprotonation of the adjacent $C(sp^2)$−H_a and $C(sp^3)$−H_b bonds furnishes allene and butadiene derivatives, respectively. The dehydration usually follows the latter pathway, because butadiene with an extended π-conjugated system is more stable than allene where two π-bonds arranged in a perpendicular manner are not conjugated. Therefore, allene has been prepared by other routes, for example, the substitution reaction of a propargyl derivative.[13] The formation of allenylidene complex **3** is in contrast to the organic counterpart, because an analogous cationic allyl species **11** is assumed to be an intermediate. The apparently unusual result can be explained by taking into account steric repulsion in the reaction intermediates and products, as summarized in Scheme 3. Protonation of the hydrolyzed form (**9**) followed by dehydration leads to the vinylcarbyne species **11** corresponding to allyl cation. When R^1 and R^2 do not bear an α-hydrogen atom, H_a is the only acidic hydrogen atom in the cationic allylic system and, therefore, deprotonation leads to the exclusive formation of allenylidene complex **3**. In the case where either R^1 or R^2 bears an α-hydrogen atom, both H_a and H_b are candidates for the subsequent deprotonation. Removal of H_b would produce alkenylvinylidene complex **5**, which corresponds to butadiene. A space-filling model of **5a**[9] is reproduced in Figure 4. When R^1 is H, as in the case of **5a**, no apparent steric repulsion between R^1 and the Cp* ring is observed. Replacement of H (R^1, shadowed) by an alkyl substituent (even a methyl group), however, would cause a

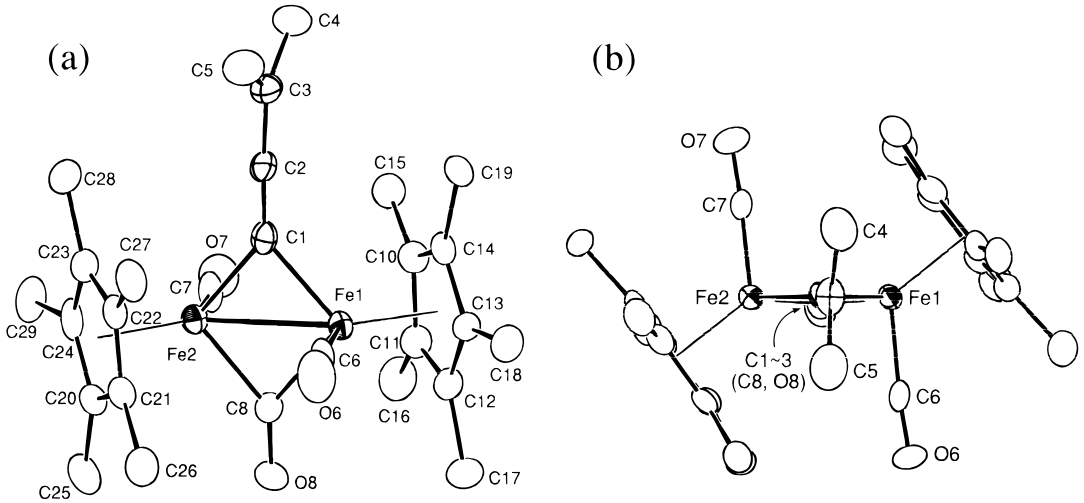

Figure 2. Molecular structure of **2b** (molecule 1) drawn at the 30% probability level. (a) overview; (b) top view.

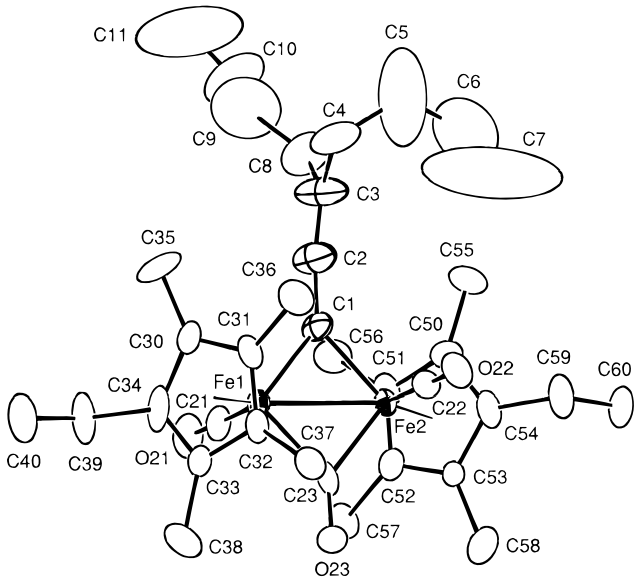

Figure 3. Molecular structure of **3c′** drawn at the 30% probability level.

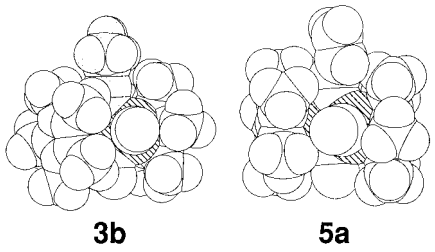

Figure 4. CPK models of **3b** and **5a**.

severe steric repulsion against the Cp* ring. Therefore, **3** may be formed as a sole product. In accord with this discussion, exclusive formation of **5** is observed only when $R^1 = H$ (eq 3) and, in addition, deprotonation of **11** by treatment with base does not produce **5** but **3**, as will be shown below.

The allenylidene skeleton in most of the previous allenylidene complexes is formed by treatment of a propargyl alcohol derivative with a metal complex, as mentioned in the Introduction. In the present case, too, the allenylidene ligand is derived from a propargyl-type structure in **8**, which is formed by a combination of (i) C−C coupling of acetylide and acyl ligands and (ii) subsequent nucleophilic addition to the acyl functional group. The final dehydration process is common for both systems to furnish the allenylidene ligand. In the present case, the dehydration is controlled by the bulky Cp* ligands, whereas formation of an alkenylvinylidene complex corresponding to **5** is frequently observed for mononuclear complexes where the dehydration process may be controlled by an electronic factor.[2]

C−C Coupling on Mononuclear Acetylide Complexes Leading to an Enone Structure. Although the formation mechanism of **2** was already discussed previously,[5d,e] some additional experiments on the C−C coupling process have been carried out. In Scheme 2, the Fp* group in **1** which is not attacked by nucleophile merely serves as an acetylide substituent by the stage of the η^2-alkyne intermediate **6**. Therefore, a similar C−C coupling reaction is expected for mononuclear acetylide complex. As typical examples, phenylacetylide complexes Fp−C≡C−Ph (**12a**; Fp = $FeCp(CO)_2$; Cp = η^5-C_5H_5) and Fp*−C≡C−Ph (**12b**) were treated with alkyllithium. As a result, styryl ketones **13** were formed in moderate yields after methanolysis, as revealed by GLC analysis (eq 4). Although the *cis*-isomer was

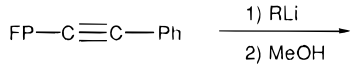

FP= Fp (**12a**), Fp* (**12b**)

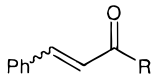

+ FP_2 (4)

13

R	Me	n-Bu	t-Bu
from **12a**	32 % (**13a**)	14 % (**13b**)	63 % (**13c**)
from **12b**	0 % (**13a**)	54 % (**13b**)	80 % (**13c**)

formed as a major product at an early stage of the reaction, it was gradually converted to the *trans*-isomer. As for organometallic products, only the dimer FP_2 was detected by TLC.

In order to obtain information on an anionic intermediate which was present before alcoholysis, a reaction mixture was treated with EtOD (eq 5). On the basis of

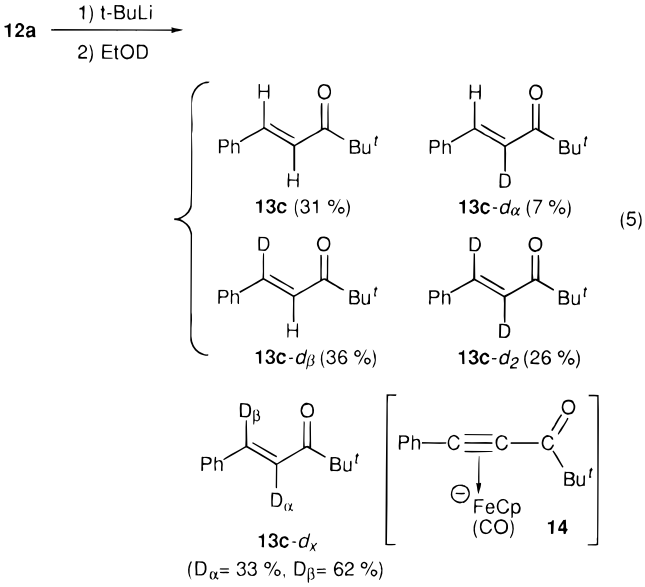

(5)

the D-distribution determined by ^{1}H-NMR analysis, an anionic intermediate **14** should be a primary organometallic product, which might be able to be trapped by PPh_3. Actually, treatment of **12** with *n*-BuLi in the presence of PPh_3 afforded an orange adduct **15** (eq 6).

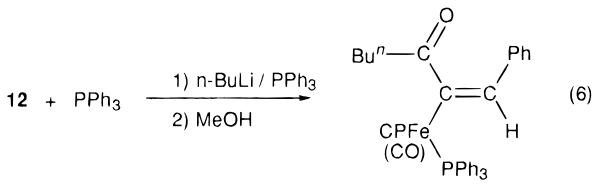

(6)

CP= Cp (**15a**) 65 %
Cp* (**15b**) 54 %

X-ray crystallography of the Cp* derivative **15b** (Figure 5 and Table 3) has revealed that it is a pentanoylstyryl complex coordinated by PPh_3.

A plausible reaction mechanism for the C−C coupling process of **12** is depicted in Scheme 4, which is similar to Scheme 2. Nucleophilic addition to a CO ligand (**12**)

Table 2. Structural Parameters for Bridging Allenylidene Complexes 3

3a		**3b** (molecule 1)		**3b** (molecule 2)		**3c′**	
			Bond Lengths (Å)				
C1−C2	1.274(7)	C1−C2	1.26(1)	C51−C52	1.26(1)	C1−C2	1.30(2)
C2−C3	1.322(9)	C2−C3	1.34(1)	C52−C53	1.38(1)	C2−C3	1.27(2)
C3−H1	0.99(6)	C3−C4	1.51(2)	C53−C54	1.46(2)	C3−C4	1.56(4)
C3−H2	0.97(6)	C3−C5	1.45(2)	C53−C55	1.50(2)	C3−C8	1.52(3)
Fe1−C1	1.946(5)	Fe1−C1	1.951(9)	Fe3−C51	1.95(1)	Fe1−C1	1.94(2)
Fe2−C1	1.937(5)	Fe2−C1	1.989(9)	Fe4−C51	1.963(9)	Fe2−C1	1.93(1)
Fe1−Fe2	2.552(1)	Fe1−Fe2	2.562(2)	Fe3−Fe4	2.561(2)	Fe1−Fe2	2.555(3)
Fe1−C4	1.736(5)	Fe1−C6	1.762(9)	Fe3−C56	1.79(1)	Fe1−C21	1.77(2)
Fe1−C6	1.934(5)	Fe1−C8	1.911(9)	Fe3−C58	1.939(9)	Fe1−C23	1.93(2)
Fe2−C5	1.733(5)	Fe2−C7	1.71(1)	Fe4−C57	1.70(1)	Fe2−C22	1.74(2)
Fe2−C6	1.939(5)	Fe2−C8	1.93(1)	Fe4−C58	1.929(9)	Fe2−C23	1.92(1)
C4−O4	1.158(5)	C6−O6	1.14(1)	C56−O56	1.13(1)	C21−O21	1.16(2)
C5−O5	1.157(5)	C7−O7	1.15(1)	C57−O7	1.19(1)	C22−O22	1.20(2)
C6−O6	1.168(5)	C8−O8	1.19(1)	C58−O58	1.17(1)	C23−O23	1.18(2)
Fe1−C10−14	2.097−2.173(5)	Fe1−C10−14	2.094−2.175(9)	Fe3−C60−64	2.120−2.167(9)	Fe1−C30−34	2.07−2.19(1)
Fe2−C20−24	2.098−2.171(5)	Fe2−C20−24	2.106−2.175(9)	Fe4−C70−74	2.098−2.179(9)	Fe2−C50−51	2.10−2.22(1)
			Bond Angles (deg)				
Fe1−C1−Fe2	82.2(2)	Fe1−C1−Fe2	81.1(4)	Fe3−C51−Fe4	81.7(4)	Fe1−C1−Fe2	82.8(6)
Fe1−C1−C2	136.8(4)	Fe1−C1−C2	139.1(7)	Fe3−C51−C52	137.2(7)	Fe1−C1−C2	138(1)
Fe2−C1−C2	141.0(4)	Fe2−C1−C2	139.8(7)	Fe4−C51−C52	141.0(8)	Fe2−C1−C2	139(1)
C1−C2−C3	178.1(7)	C1−C2−C3	176(1)	C51−C52−C53	177(1)	C1−C2−C3	172(2)
C2−C3−H1	113(4)	C2−C3−C4	123(1)	C52−C53−C54	123(1)	C2−C3−C4	125(2)
C2−C3−H2	114(4)	C2−C3−C5	126(1)	C52−C53−C55	122(1)	C2−C3−C8	123(2)
H1−C3−H2	132(6)	C4−C3−C5	111(1)	C54−C53−C55	115(1)	C4−C3−C8	111(2)
Fe2−Fe1−C1	48.8(1)	Fe2−Fe1−C1	50.1(3)	Fe4−Fe3−C51	49.3(3)	Fe2−Fe1−C1	48.4(4)
Fe2−Fe1−C4	96.3(1)	Fe2−Fe1−C6	95.3(3)	Fe4−Fe3−C56	95.5(3)	Fe2−Fe1−C21	95.8(5)
Fe2−Fe1−C6	48.9(1)	Fe2−Fe1−C8	48.5(3)	Fe4−Fe3−C58	48.4(3)	Fe2−Fe1−C23	48.4(4)
C1−Fe1−C4	92.4(2)	C1−Fe1−C6	92.4(4)	C51−Fe3−C56	91.7(4)	C1−Fe1−C21	95.5(7)
C1−Fe1−C6	97.6(2)	C1−Fe1−C8	98.5(4)	C51−Fe3−C58	97.6(4)	C1−Fe1−C23	96.7(6)
Fe1−Fe2−C1	49.1(1)	Fe1−Fe2−C1	48.8(3)	Fe3−Fe4−C51	49.0(3)	Fe1−Fe2−C1	48.8(5)
Fe1−Fe2−C5	96.4(1)	Fe1−Fe2−C7	94.5(3)	Fe3−Fe4−C57	96.1(3)	Fe1−Fe2−C22	96.3(5)
Fe1−Fe2−C6	48.7(1)	Fe1−Fe2−C8	47.8(3)	Fe3−Fe4−C58	48.7(3)	Fe1−Fe2−C23	48.7(5)
C1−Fe2−C5	93.5(2)	C1−Fe2−C7	96.5(4)	C51−Fe4−C57	96.7(4)	C1−Fe2−C22	93.2(7)
C1−Fe2−C6	97.7(2)	C1−Fe2−C8	96.5(4)	C51−Fe4−C58	97.6(4)	C1−Fe2−C23	97.5(7)
Fe1−C4−O4	176.1(4)	Fe1−C6−O6	175.4(9)	Fe3−C56−O56	175.6(8)	Fe1−C21−O21	176(1)
Fe2−C5−O5	175.1(4)	Fe2−C7−O7	173.3(9)	Fe4−C57−O57	176.2(9)	Fe2−C22−O22	177(1)
Fe1−C6−O6	138.9(4)	Fe1−C8−O8	138.7(7)	Fe3−C58−O58	137.6(8)	Fe1−C23−O23	138(1)
Fe2−C6−O6	138.7(4)	Fe2−C8−O8	137.5(7)	Fe4−C58−O58	139.4(7)	Fe2−C23−O23	139(1)

followed by C−C coupling leads to the anionic η^2-alkyne complex-type intermediate **16**. A small amount of Ph−C≡C−C(=O)−*n*-Bu which leaked from the reaction sequence was detected by GC-MS analysis of the reaction mixture. Protonation of **16** initially takes place at the β-carbon atom to give the coordinatively unsaturated α-acylstyryl intermediate **17**, where the Fe−C bond is protonated under the reaction conditions to furnish the styryl ketone **13**. In the presence of PPh_3, coordination to the Fe center in **16** and protonation of the resulting carbanionic species **18** gives **15**. Thus it has been revealed that an enone structure can be built by treatment of iron acetylide with a nucleophile and via C−C coupling of an acyl−acetylide intermediate.

Formation of Diacylvinylidene Complex 4 by Addition of an Excess Amount of *n*-BuLi to 1 in One Portion. In contrast to the one-pot synthesis of **3**, addition of nucleophile (*n*-BuLi) to **1** *in one portion* did not produce **3**, but the diacylvinylidene complex **4** was produced in a low yield (eq 7). NMR spectra

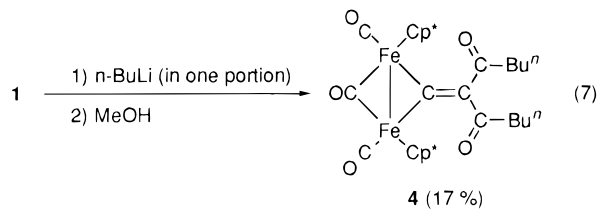

(7)

Chart 2

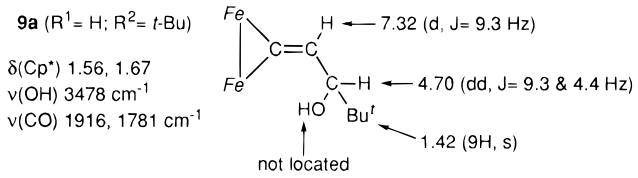

Table 3. Selected Structural Parameters for 15b

	Interatomic Distances (Å)		
Fe−P	2.233(5)	O14−C14	1.17(2)
Fe−C1	2.01(1)	C1−C2	1.35(2)
Fe−C14	1.74(2)	C1−C9	1.51(2)
Fe−C20−24	2.12−2.20(2)	C2−C3	1.49(2)
O9−C9	1.20(2)	C9−C10	1.50(2)
	Bond Angles (deg)		
P−Fe−C1	92.6(5)	C2−C3−C4	119(2)
P−Fe−C14	88.8(6)	C2−C3−C8	122(1)
C1−Fe−C14	92.9(8)	C4−C3−C8	119(1)
Fe−C1−C2	125(1)	O9−C9−C1	122(2)
Fe−C1−C9	114(1)	O9−C9−C10	122(2)
C2−C1−C9	121(1)	C1−C9−C10	115(2)
C1−C2−C3	128(1)	Fe−C14−O14	175(2)

containing single Cp* and *n*-BuCO resonances indicated a symmetrical structure, which has been characterized by X-ray crystallography (Figure 6 and Table 4; for structural discussion, see below). At the present time, little information about its formation mechanism is available. At least it is evident that an intermolecular step should be involved, because the number of CO functional groups is increased from 4 (**1**) to 5 (**4**).

Scheme 2

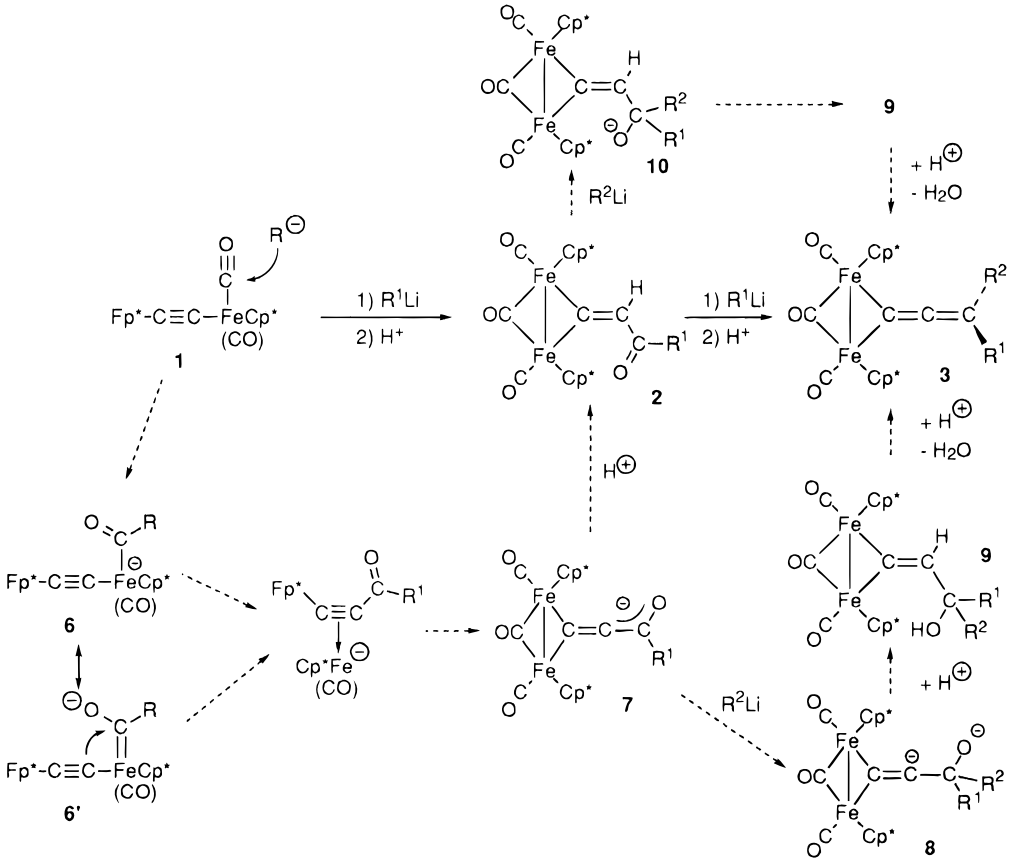

Reaction of 3 with H^+ (an Electrophile) Leading to the Cationic Vinylcarbyne Complex 11. It has been established that vinylidene complexes react with electrophiles (E) at the β-carbon atom to give carbyne species $M_n[\equiv C-C(E)R_2]$.[1] Addition of CF_3SO_3H or $HBF_4 \cdot OEt_2$ to the diiron bridging allenylidene complex **3** produced cationic μ-vinylcarbyne complex **11** as a single species, as observed by NMR (eq 8).

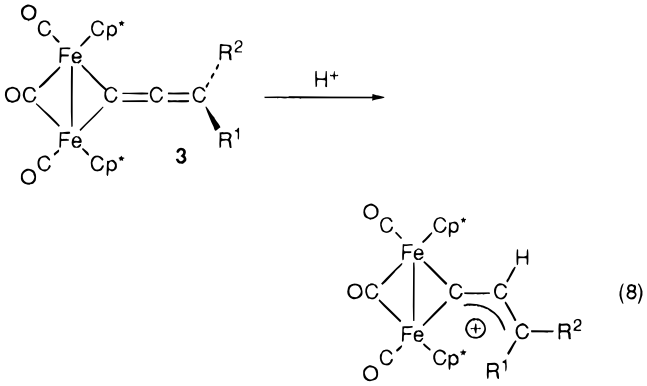

(8)

	R^1	R^2	
11a	H	H	(from **3a**)
11b	Me	Me	(from **3b**)
11c	H	Ph	(from **3d**)

Complex **11** is readily characterized on the basis of its NMR data. The ^{1}H-NMR spectrum of **11a** contains a typical vinyl pattern, i.e., three protons coupled with each other (Chart 3), clearly indicating that a proton is attached to the β-carbon atom in **3**. A similar coupling pattern is observed for **11c** (δ_H 6.95, 9.31 (J_{HH} = 15.6 Hz)) with a *trans*-configuration, which has been confirmed by X-ray crystallography (see below). The most characteristic spectral feature is the highly deshielded quaternary carbon signal due to the α-carbon atom (δ_C 500.9 (**11a**),[14] 455.9 (**11b**), 452.0 (**11c**)). Recently, Etienne reported a similar protonation of the dicyano derivative $Cp_2Fe_2[\mu\text{-}C{=}C{=}C(CN)_2](\mu\text{-}CO)(dppe)$, leading to the corresponding cationic vinylcarbyne species $[Cp_2Fe_2[\mu\text{-}\{C-C(H)-C\}^+(CN)_2](\mu\text{-}CO)(dppe)]$.[3a] Related Cp derivatives were synthesized by γ-hydride abstraction from the corresponding diiron bridging vinylidene complex or dehydrative coupling between a cationic μ-methylidyne complex $[Cp_2Fe_2(\mu\text{-}CH)(\mu\text{-}CO)(CO)_2]^+$ and ketone (or aldehyde), as reported by Casey et al.[8] The α-carbon signals of these complexes are similarly located in the highly deshielded region.

The molecular structure of the Ph derivative **11c** (BF_4 salt) has been determined by X-ray crystallography (Figure 7 and Table 5). However, the allylic part is almost completely disordered, and the structure has been refined by using two components of equal occupancy factors (C2a−C3a:C2b−C3b = 0.5:0.5). Therefore, the structural features, in particular the relative

(13) Brandsma, L. *Synthesis of Acetylenes, Allenes and Cumulenes*; Elsevier: Amsterdam, 1981.

(14) Despite of several attempts (in CD_2Cl_2 and CD_3NO_2, from room temperature to −80 °C), the β- and γ-carbon atom signals could not be located.

Scheme 3

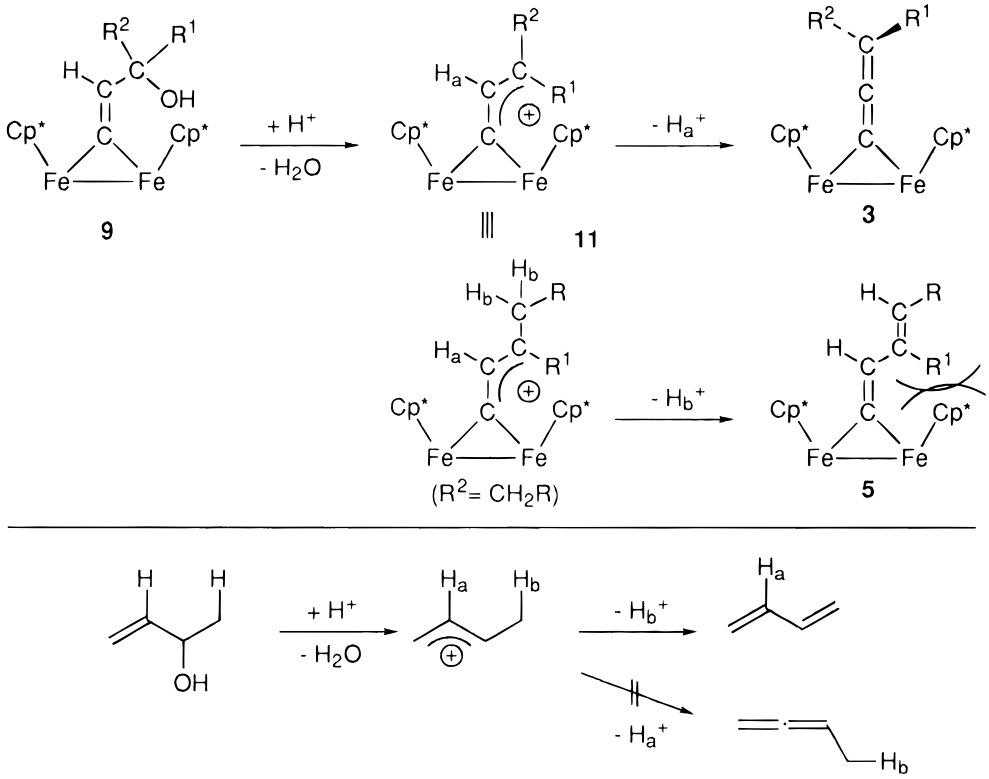

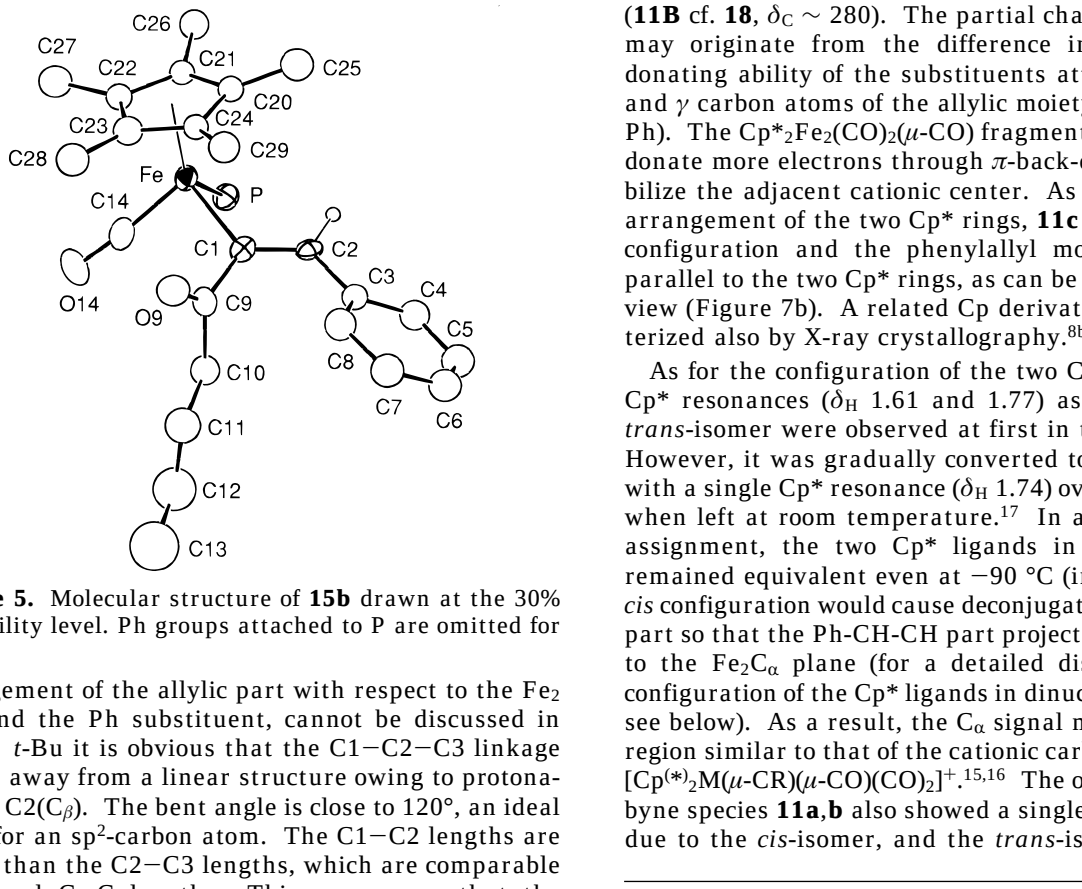

Figure 5. Molecular structure of **15b** drawn at the 30% probability level. Ph groups attached to P are omitted for clarity.

arrangement of the allylic part with respect to the Fe_2 core and the Ph substituent, cannot be discussed in detail. *t*-Bu it is obvious that the C1−C2−C3 linkage is bent away from a linear structure owing to protonation at C2(C_β). The bent angle is close to 120°, an ideal angle for an sp^2-carbon atom. The C1−C2 lengths are longer than the C2−C3 lengths, which are comparable to normal C=C lengths. This may mean that the cationic charge does not completely delocalize over the allylic part; in other words, C_α bears a more cationic character (see **11A** in eq 8). In accord with this discussion, the $\delta_C(C_\alpha)$ value is closer to that of cationic μ-carbyne species $[Cp^{(*)}_2M(\mu\text{-CR})(\mu\text{-CO})(CO)_2]^+$ (δ_C > 450; M= Fe,[15] Ru[16]) than to that of μ-vinylidene species (**11B** cf. **18**, $\delta_C \sim 280$). The partial charge localization may originate from the difference in the electron-donating ability of the substituents attached to the α and γ carbon atoms of the allylic moiety (Fe_2 vs H and Ph). The $Cp^*_2Fe_2(CO)_2(\mu\text{-CO})$ fragment may be able to donate more electrons through π-back-donation to stabilize the adjacent cationic center. As for the relative arrangement of the two Cp* rings, **11c** adopts a *trans*-configuration and the phenylallyl moiety is located parallel to the two Cp* rings, as can be seen from a top view (Figure 7b). A related Cp derivative was characterized also by X-ray crystallography.[8b]

As for the configuration of the two Cp* ligands, two Cp* resonances (δ_H 1.61 and 1.77) assignable to the *trans*-isomer were observed at first in the case of **11c**. However, it was gradually converted to the *cis*-isomer with a single Cp* resonance (δ_H 1.74) over a 12 h period when left at room temperature.[17] In accord with this assignment, the two Cp* ligands in the *cis*-isomer remained equivalent even at −90 °C (in CD_2Cl_2). The *cis* configuration would cause deconjugation of the allylic part so that the Ph-CH-CH part projects perpendicular to the Fe_2C_α plane (for a detailed discussion of the configuration of the Cp* ligands in dinuclear complexes, see below). As a result, the C_α signal may appear in a region similar to that of the cationic carbyne complexes $[Cp^{(*)}_2M(\mu\text{-CR})(\mu\text{-CO})(CO)_2]^+$.[15,16] The other μ-vinylcarbyne species **11a**,**b** also showed a single Cp* resonance due to the *cis*-isomer, and the *trans*-isomer could not

(15) Casey, C. P.; Fagan, P.; Miles, W. H. *J. Am. Chem. Soc.* **1982**, *104*, 1134.

(16) Colborn, R. E.; Davies, D. L.; Dyke, A. F.; Endesfelder, A.; Knox, S. A. R.; Orpen, A. G.; Plaas, D. *J. Chem. Soc., Dalton Trans.* **1983**, 2661.

(17) Crystals of **11c** dissolved in $CDCl_2$ also showed a single resonance. Although this result is not consistent with that of the X-ray crystallography, the single crystal that was picked for X-ray diffraction might have been the *trans*-isomer.

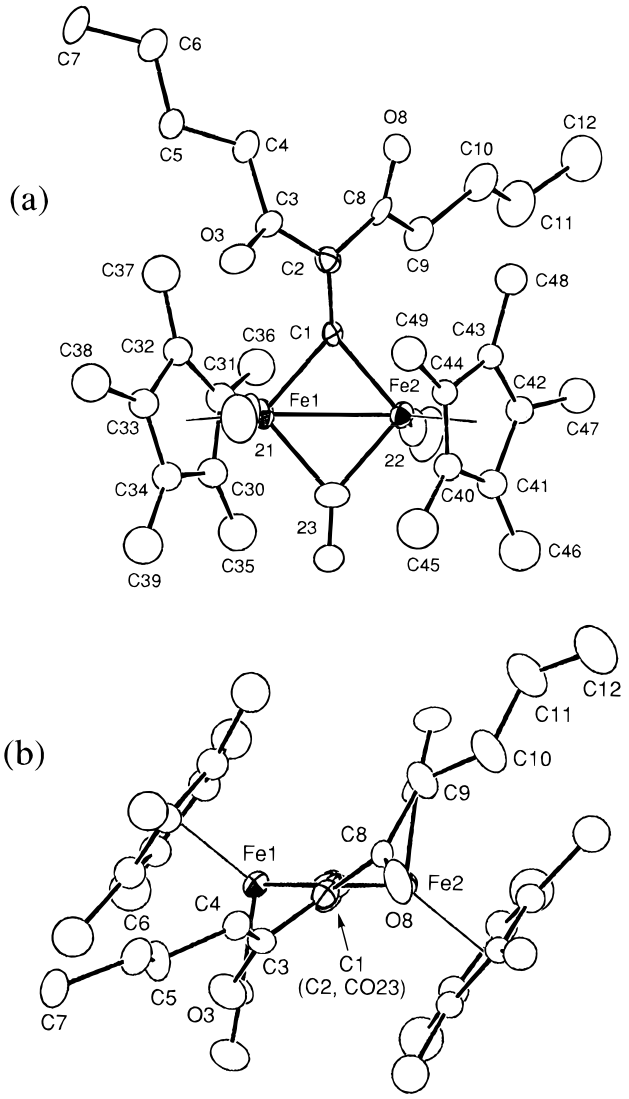

Figure 6. Molecular structure of **4** drawn at the 30% probability level. (a) overview.; (b) side view. (Numbers without atom names are for CO ligands.)

be detected by ^{1}H-NMR monitoring of the reaction mixtures. The less bulky vinyl part, CH−CH$_2$ (**11a**) and CH−CMe$_2$ (**11b**), might result in rapid isomeization via flipping of a Cp* ligand.

The protonation is found to be reversible.[3a] Treatment of **11a**,**b** with **a** less nucleophilic base such as 2,6-lutidine, and proton sponge regenerated the allenylidene complexes **3a**,**b** (eq 9). Complex **11b** was also deprotonated by HNEt$_2$, though nucleophilic addition was observed in the case of the reaction with **11a**, as described below.

11a,b —(2,6-lutidine or proton sponge)→ **3a,b** (9)

Thus, the proton (electrophile) attacks the β-carbon atom, which is also the reaction site of bridging vinylidene complexes upon treatment with electrophiles. We also attempted the reaction with other electrophiles, such as alkylating reagent (Me−OSO$_2$CF$_3$) and transition metal electrophile [Fp$^+$(THF)BF$_4$], but no reaction took place, probably because of the steric shielding of the β-carbon atom by the Cp* ligands.

Nucleophilic Addition to Cationic Vinylcarbyne Complex 11 Giving Functionalized Vinylidene Complex 18. Cationic vinylcarbyne complex **11** is susceptible to nucleophilic addition. Addition of Et$_4$NBH$_4$, a hydride source, to a CH$_2$Cl$_2$ solution of **11** afforded vinylidene complex **18** via hydride transfer to the γ-carbon atom (eq 10). Isolation of **11** was not a requisite process, and sequential addition of H$^+$, nucleophile, and MeOH to **3** furnished the desired vinylidene complex **18**. Addition of too much Et$_4$NBH$_4$ resulted in reduction of the vinylidene functional group to give μ-alkylidene complex **19** (eq 11). The μ-propenylidene complex **19a** has been characterized by X-ray crystallography (Figure 8 and Table 6).

3a,b —(1) H$^+$; (2) Et$_4$NBH$_4$ or LiCuR$_2$ (*Nu*); (3) MeOH; in ether or THF→ **18** (10)

	R^1	R^2	*Nu*	Yield
18a	H	H	H	41
18b	H	H	Me	23
18c	H	H	Bu^n	18
18d	H	H	Ph	30
18e	Me	Me	H	41
18f	Me	Me	Me	60
18g	Me	Me	Bu^n	37
18h	Me	Me	Ph	46
18i	H	Ph	Ph	27
18j	H	H	NEt$_2$	31 (in acetone)

3b,c —(1) H$^+$; (2) Et$_4$NBH$_4$ (excess); (3) MeOH; in CH$_2$Cl$_2$→ (11)

R= H (**19a**); Ph (**19b**).

Although attempted alkylation with RLi was unsuccessful (a low yield mixture of products containing **18** was obtained), reaction of lithium dialkylcuprate resulted in alkylation at the γ-carbon atom to give a variety of substituted vinylidene complexes **18** (eq 10), which were readily characterized on the basis of the quaternary carbon signals appearing around 280 ppm. Treatment of **3a** with HNEt$_2$ produced the aminated compound **18j**.

The molecular structure of **18e**,**h** has been determined by X-ray crystallography, and ORTEP views are shown in Figures 9 and 10. Their structural parameters are summarized in Table 4, together with the diacyl−vinylidene complex **4** and the related vinylidene complex **18k** (R^1 = R^2 = Me, Nu = Cp*; see below).

The γ-attack appears to be in contrast to the above consideration on the structure and the ^{13}C-NMR chemical shifts of the allylic part of **11**, suggesting that the α-carbon atom is the most electrophilic site. But, as far as we are aware, α-attack has never been observed for our and related systems. In particular, in the present case, the α-carbon atom is sterically protected from any addition by the Cp* rings, as typically exemplified by the CPK models of the related compounds (Figure 4).

Table 4. Structural Parameters for Bridging Vinylidene Complexes 4 and 18

4		18e		18h		18k	
			Bond Lengths (Å)				
C1−C2	1.34(2)	C1−C2	1.31(1)	C1−C2	1.33(3)	C1−C2	1.333(8)
C2−C3	1.49(2)	C2−C3	1.50(1)	C2−C3	1.56(3)	C2−C3	1.49(1)
C2−C8	1.49(2)	C2−H1	0.95(6)			C2−H2	0.97(5)
C3−C4	1.49(2)	C3−C4	1.54(1)	C3−C4	1.60(3)	C3−H3a	
C8−C9	1.48(2)	C3−C5	1.51(1)	C3−C5	1.58(3)	C3−H3b	
C3−O3	1.21(1)	C3−H2	0.82(6)	C3−C31	1.42(3)	C3−C30	1.542(9)
C8−O8	1.25(2)						
Fe1−Fe2	2.533(3)	Fe1−Fe2	2.566(2)	Fe1−Fe2	2.559(6)	Fe1−Fe2	2.561(2)
Fe1−C1	1.93(1)	Fe1−C1	1.918(8)	Fe1−C1	1.97(3)	Fe1−C1	1.931(7)
Fe2−C1	1.93(1)	Fe2−C1	1.969(8)	Fe2−C1	1.94(2)	Fe2−C1	1.922(7)
Fe1−C21	1.81(2)	Fe1−C6	1.735(9)	Fe1−C6	1.75(3)	Fe1−C4	1.750(8)
Fe1−C22	1.95(2)	Fe1−C8	1.955(7)	Fe1−C8	1.97(3)	Fe1−C6	1.917(7)
Fe2−C23	1.73(2)	Fe2−C7	1.726(9)	Fe2−C7	1.69(3)	Fe2−C5	1.760(8)
Fe2−C22	1.93(2)	Fe2−C8	1.920(8)	Fe2−C8	1.89(3)	Fe2−C6	1.908(7)
O21−C21	1.12(2)	O6−C6	1.161(9)	O6−C6	1.15(3)	O4−C4	1.151(8)
O22−C22	1.17(4)	O7−C7	1.170(9)	O7−C7	1.23(3)	O5−C5	1.145(8)
O23−C23	1.14(2)	O8−C8	1.170(8)	O8−C8	1.17(3)	O6−C6	1.197(7)
Fe1−C30−34	2.12−2.19(2)	Fe1−C10−14	2.120−2.173(8)	Fe1−C10−14	2.07−2.22(3)	Fe1−C10	2.128−2.193(7)
Fe2−C40−44	2.11−2.19(2)	Fe2−C20−24	2.103−2.175(8)	Fe2−C20−24	2.10−2.21(3)	Fe2−C20	2.125−2.196(7)
			Bond Angles (deg)				
Fe2−Fe1−C1	48.9(4)	Fe2−Fe1−C1	49.6(2)	Fe2−Fe1−C1	48.6(7)	Fe2−Fe1−C1	48.2(2)
Fe2−Fe1−C21	97.4(5)	Fe2−Fe1−C6	97.1(3)	Fe2−Fe1−C6	96(1)	Fe2−Fe1−C4	96.0(3)
Fe2−Fe1−C22	48.8(5)	Fe2−Fe1−C8	48.0(2)	Fe2−Fe1−C8	47.2(8)	Fe2−Fe1−C6	47.8(2)
C1−Fe1−C21	94.6(7)	C1−Fe1−C6	89.4(4)	C1−Fe1−C6	94(1)	C1−Fe1−C4	90.9(3)
C1−Fe1−C22	97.7(6)	C1−Fe1−C8	97.4(3)	C1−Fe1−C8	95(1)	C1−Fe1−C6	96.0(3)
C21−Fe1−C22	94.7(7)	C6−Fe1−C8	96.4(4)	C6−Fe1−C8	92(1)	C4−Fe1−C6	96.9(3)
Fe1−Fe2−C1	49.0(4)	Fe1−Fe2−C1	47.8(2)	Fe1−Fe2−C1	49.6(8)	Fe1−Fe2−C1	48.5(2)
Fe1−Fe2−C23	96.6(5)	Fe1−Fe2−C7	94.2(3)	Fe1−Fe2−C7	96(1)	Fe1−Fe2−C5	95.0(2)
Fe1−Fe2−C22	49.6(5)	Fe1−Fe2−C8	49.1(2)	Fe1−Fe2−C8	49.8(9)	Fe1−Fe2−C6	48.1(2)
C1−Fe2−C23	99.9(7)	C1−Fe2−C7	90.7(4)	C1−Fe2−C7	90(1)	C1−Fe2−C5	90.0(3)
C1−Fe2−C22	98.5(6)	C1−Fe2−C8	96.8(3)	C1−Fe2−C8	99(1)	C1−Fe2−C6	96.6(3)
C22−Fe2−C23	89.1(8)	C7−Fe2−C8	98.5(4)	C7−Fe2−C8	98(1)	C5−Fe2−C6	97.0(3)
Fe1−C1−Fe2	82.1(5)	Fe1−C1−Fe2	82.6(3)	Fe1−C1−Fe2	82(1)	Fe1−C1−Fe2	83.3(3)
Fe1−C1−C2	134(1)	Fe1−C1−C2	145.4(7)	Fe1−C1−C2	146(2)	Fe1− C1−C2	141.8(6)
Fe2−C1−C2	142(1)	Fe2−C1−C2	131.8(6)	Fe2−C1−C2	132(2)	Fe2−C1−C2	134.8(5)
C1−C2−C3	123(1)	C1−C2−C3	130.1(8)	C1−C2−C3	135(2)	C1−C2−C3	129.1(7)
C1−C2−C8	120(1)	C1−C2−H1	124(4)			C1−C2−H2	118(3)
		C3−C2−H1	106(4)			C3−C2−H2	113(3)
Fe1−C21−O21	174(2)	Fe1−C6−O6	176.5(9)	Fe1−C6−O6	173(3)	Fe1− C4−O4	176.7(8)
Fe2−C23−O23	173(1)	Fe2−C7−O7	175.3(8)	Fe2−C7−O7	179(2)	Fe2−C5−O5	176.7(7)
Fe1−C22−Fe2	81.6(6)	Fe1−C8−Fe2	82.9(3)	Fe1−C8−Fe2	83(1)	Fe1−C6−Fe2	84.1(3)
Fe1−C22−O22	136(2)	Fe1−C8−O8	137.2(6)	Fe1−C8−O8	135(2)	Fe1−C6−O6	139.1(6)
Fe2−C22−O22	141(1)	Fe2−C8−O8	139.8(6)	Fe2−C8−O8	141(2)	Fe2−C6−O6	136.8(6)

We also attempted metalation of **11a**,**c** by treatment with Na[FeCp(CO)$_2$], Et$_4$N[MoCp(CO)$_3$], PPN[Co(CO)$_4$], and PPN[Mn(CO)$_5$], but the μ-propenylidene complex **18a** was obtained probably via an electron-transfer process. In the case of **11c**, deprotonation was also observed as a side reaction.

Comparison of the Structure of Diiron Complexes Cp*$_2$Fe$_2$[μ-(C=)$_m$CR$_2$](μ-CO)(CO)$_2$ 3 (m = 2), 4, 18 (m = 1) and 19 (m = 0). A series of Cp*$_2$Fe$_2$(μ-X)(μ-CO)(CO)$_2$-type diiron complexes containing bridging allenylidene (**3**), vinylidene (diacyl-substitued (**4**), mono primary-alkyl-substituted (**18k**, see below), mono secondary-alkyl-substituted (**18e**), mono tertiary-alkyl-substituted (**18h**)), and alkylidene ligands (**19a**) are obtained by the present study. We also have a crystal structure of the η^5-C$_5$Me$_4$Et derivative of a parent vinylidene complex (η^5-C$_5$Me$_4$Et)$_2$Fe$_2$(CO)$_2$(μ-CO)(μ-C=CH$_2$) (**18l**).[18] Here, we would like to discuss their structures with the emphasis on (i) the steric repulsion between the bridging ligand and the Cp* rings and (ii) the relative arrangement of the two Cp* ligands (*cis* or *trans*).

In the case of the allenylidene complexes **3a**−**c**, no apparent steric interaction between the substituents at C$_\gamma$ and the Cp* rings is observed, as discussed above, mainly because the C$_\gamma$R$_2$ moiety is far from the sterically congested Fe$_2$Cp*$_2$ core and the γ-substituents project to the space where the Cp* ligands do not project. Therefore, the Cp* rings are arranged in a *trans*-

(18) Complex **18l** was prepared following the procedure described in ref 5c. Crystal data: C$_{27}$H$_{36}$O$_3$Fe$_2$, mw = 520.3, monoclinic, space group *C*2/*m*, *a* = 11.673(4) Å, *b* = 12.490(3) Å, *c* = 9.391(3) Å, β = 115.88(2)°, *V* = 1231.8(7) Å^3, *Z* = 2, d_{calcd} = 1.40 g·cm^{-3}, *R* (*R*$_w$) = 0.039 (0.090) for 1213 unique data with $I > 3\sigma(I)$ and 127 variables. The structure which was imposed not only on a centrosymmetric site but also on a mirror-symmetric site was found to be completely disordered with respect to the midpoint of the Fe−Fe bond and the two mirror planes bisecting the structure, and the bridging carbon atoms for the two bridging ligands (C1 and C1*) could not be resolved. Important bond lengths (Å) and angles (deg): Fe1−Fe1* 2.547(1), Fe1−C1 1.920(3), C1−C2 1.38(6), C2−H2 0.91(4), C1*−O2* 1.13(4) , Fe1−C1−Fe1* 83.1(2), Fe1−C1−C2 138.45(9), C1−C2−H2 118(4), H2−C2−H2* 123(8), Fe1−C1*−O2* 138.45(9).

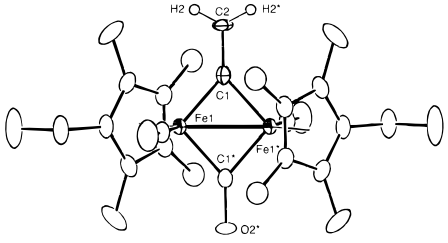

Scheme 4

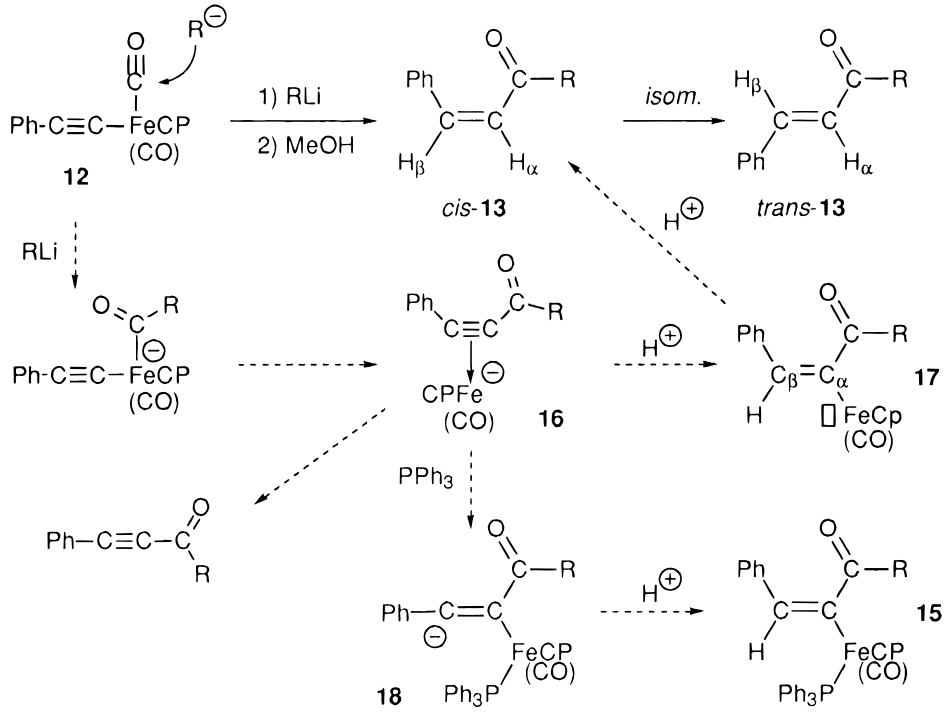

Chart 3

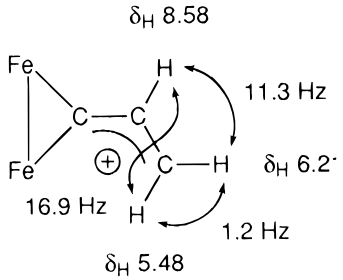

configuration, so as to minimize steric repulsion between them.

On the other hand, the C_β substituents of the μ-vinylidene complexes **4** and **18** project toward the Cp* rings. Therefore, they have to reduce steric repulsion by some distortion. The structural parameters for the core parts of the vinylidene and allenylidene complexes are summarized in Table 7. First of all, no systematic difference between the two Fe−C1 bond lengths (entries 1 and 2) is observed irrespective of the symmetry of the structures. In the case of the parent vinylidene complex **18l**, no apparent steric repulsion is observed. For example, the C1═C2−H2 angle of 118(4)° falls in the typical range of those for an olefinic functional group and the CH_2 triangle is coplanar with the Fe_2C triangle (entries 15 and 16), although the latter feature comes from the crystallographic requirement of a centric space group. In the series of the monosubstituted derivatives **18e**,**h**,**k**, the Fe1−C1−C2−C3 linkage stretches so as to minimize the steric repulsion between the β-alkyl substituent (R_β) and the Cp* group attached to Fe1. For example, the Fe1−C1−C2 and C1−C2−C3 angles (entries 4 and 7) and their sum (entry 8) increase as R_β becomes more bulky from a primary alkyl group (CH_2-Cp*) to a secondary alkyl group ($CHMe_2$) and then to a tertiary alkyl group (CMe_2Ph). At the same time, the C1−C2 part is tilted toward Fe2. The Fe1−C1−C2 angles are larger than the Fe2−C2−C3 angles by 7° (**18k**), 14° (**18e**), and 14° (**18h**) (entry 6), while the difference of the corresponding angles in the allenylidene complexes **3** is less than 4°. The Cp* rings are also bent away from the vinylidene bridge. All the Fe−Fe−cp angles for **18** and **3** fall in the narrow range of 138.1−142.8° (entries 9 and 10), but a significant difference has been observed for the dihedral angles between the Fe_2C and Fe_2cp planes (torsion angles are shown in entries 11 and 12; cp stands for centroid of a Cp* ligand). In general, dihedral angles for the μ-vi-

Table 5. Selected Structural Parameters for 11c

Interatomic Distances (Å)			
Fe1−C1	1.814(5)	C34−C35	1.342(9)
Fe2−C1	1.830(6)	C35−C36	1.381(8)
C1−C2a	1.51(2)	Fe1−Fe2	2.524(1)
C2a−C3a	1.33(2)	Fe1−C10−14	2.120−2.156(6)
C3a−C31	1.49(2)	Fe2−C20−24	2.108−2.172(6)
C1−C2b	1.44(2)	Fe1−C4	1.778(6)
C2b−C3b	1.31(2)	Fe1−C6	1.938(5)
C3b−C31	1.54(2)	Fe2−C5	1.746(7)
C31−C32	1.360(9)	Fe2−C6	1.936(6)
C31−C36	1.361(9)	O4−C4	1.132(6)
C32−C33	1.385(9)	O5−C5	1.153(7)
C33−C34	1.356(9)	O6−C6	1.161(6)

Bond Angles (deg)			
Fe1−C1−Fe2	87.7(2)	C33−C34−C35	118.6(7)
Fe1−C1−C2a	125.7(6)	C34−C35−C36	121.2(7)
Fe2−C1−C2a	143.0(6)	C31−C36−C35	120.6(7)
C1−C2a−C3a	116(2)	Fe2−Fe1−C1	46.4(2)
C2a−C3a−C31	117(2)	Fe2−Fe1−C4	97.3(2)
C3a−C31−C32	100.9(9)	Fe2−Fe1−C6	49.3(2)
C3a−C31−C36	140.8(9)	C1−Fe1−C4	95.0(3)
Fe1−C1−C2b	143.4(6)	C1−Fe1−C6	95.7(2)
Fe2−C1−C2b	123.7(7)	C4−Fe1−C6	93.6(2)
C1−C2b−C3b	119(2)	Fe1−Fe2−C1	45.9(2)
C2b−C3b−C31	119(2)	Fe1−Fe2−C5	97.2(2)
C3b−C31−C32	137.3(9)	C1−Fe2−C6	95.3(2)
C3b−C31−C36	104.4(9)	C5−Fe2−C6	97.2(3)
Fe1−Fe2−C6	49.4(2)	Fe1−C4−O4	177.3(6)
C1−Fe2−C5	93.8(3)	Fe2−C5−O5	176.6(8)
C32−C31−C36	118.3(6)	Fe1−C6−Fe2	81.3(2)
C31−C32−C33	120.5(7)	Fe1−C6−O6	138.5(5)
C32−C33−C34	120.8(7)	Fe2−C6−O6	140.2(5)

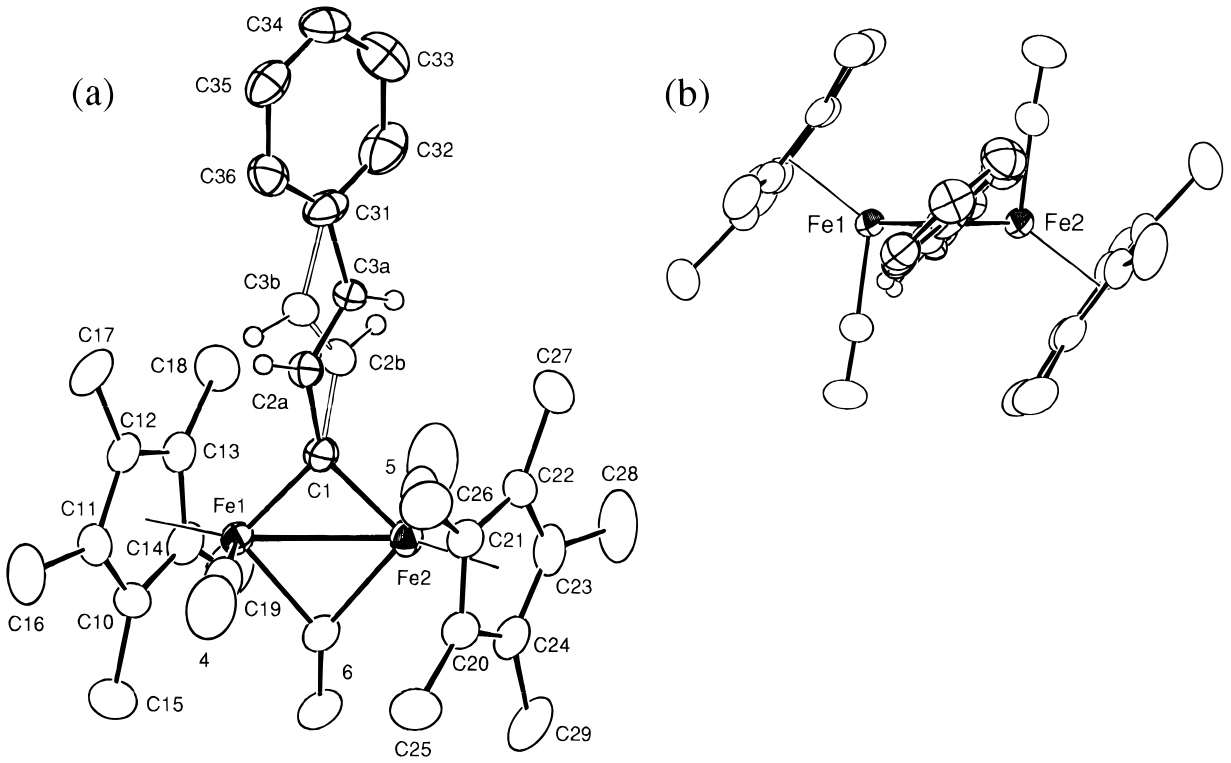

Figure 7. Structure of the cationic part **11c** drawn at the 30% probability level: (a) overview; (b) top view. (Numbers without atom names are for CO ligands.)

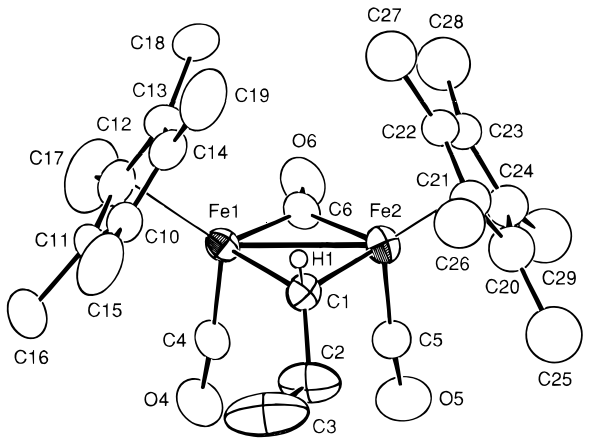

Figure 8. Molecular structure of **19a** drawn at the 30% probability level.

Table 6. Selected Structural Parameters for 19

Interatomic Distances (Å)			
C1−C2	1.50(1)	Fe1−C6	1.914(8)
C2−C3	1.36(2)	Fe1−C10−14	2.115−2.174(10)
O4−C4	1.16(1)	Fe2−C1	1.970(8)
O5−C5	1.14(1)	Fe2−C5	1.739(9)
O6−C6	1.188(9)	Fe2−C6	1.923(8)
Fe1−Fe2	2.572(2)	Fe2−C20−24	2.130−2.311(7)
Fe1−C1	1.989(8)	Fe2−C30−34	2.14−2.15(1)
Fe1−C4	1.714(9)		

Bond Angles (deg)			
Fe1−C1−Fe2	81.0(3)	Fe2−Fe1−C6	48.1(2)
Fe1−C1−C2	125.1(6)	C1−Fe1−C4	91.8(4)
Fe2−C1−C2	119.8(6)	C1−Fe1−C6	97.0(3)
C1−C2−C3	121.8(9)	C4−Fe1−C6	90.3(4)
Fe1−C4−O4	175.4(8)	Fe1−Fe2−C1	49.8(2)
Fe2−C5−O5	174.2(8)	Fe1−Fe2−C5	94.7(3)
Fe1−C6−Fe2	84.2(3)	Fe1−Fe2−C6	47.8(2)
Fe1−C6−O6	139.1(7)	C1−Fe2−C5	92.6(4)
Fe2−C6−O6	136.8(7)	C1−Fe2−C6	97.3(3)
Fe2−Fe1−C1	49.2(2)	C5−Fe2−C6	88.4(4)
Fe2−Fe1−C4	95.6(3)		

nylidene complex are larger than those for the μ-allenylidene complexes, as typically exemplified by the sum of the angles (entry 14). In addition, the difference (entry 13) increases as R_β becomes more bulky. Thus, Cp* ligands also minimize the steric repulsion by precession around the Fe−Fe axis.

However, the tendency observed for the above-mentioned parameters is not always as monotonous as going from a primary alkyl substituent to a tertiary alkyl substituent and to a disubstituted derivative. In the case of the sterically congested complexes such as **18h** with a tertiary substituent and the disubstituted complex **4**, the steric repulsion is also reduced by a twisting of the vinylidene moiety, as can be seen from the top views (Figures 6b and 9b). The extent of twisting can be estimated by the torsion angles of Fe1−C1−C2−C3 and Fe1−C1−C2−X (the other C_β-substituent) (entries 15 and 16). Those for **18h** and **4** are considerably larger than those for **18k** and **18e**. The twisting also causes elongation of the Fe−C1 distances (entries 1 and 2) because an increased torsion angle leads to a decreased Fe−C1 orbital overlap.

Thus, μ-vinylidene complexes reduce the steric repulsion between the vinylidene substituents and Cp* ligands by a combination of a stretching and twisting of the vinylidene moiety and precession of the Cp* ligands.

As for μ-alkylidene complexes, the bridging carbon atom which bears two substituents lies closer to the Fe_2-Cp^*_2 core than C_β in the μ-vinylidene complex does, but they project to the less congested space (perpendicular to the Fe−Fe vector). On the basis of the many examples of $(\eta^5\text{-}C_5R_5)Fe_2(\mu\text{-}CXY)(\mu\text{-}CO)(CO)_2$-type complexes (R = H, Me), the following conclusions concerning the stereochemistry with respect to the $Fe_2(\mu\text{-}C)(\mu\text{-}CO)$

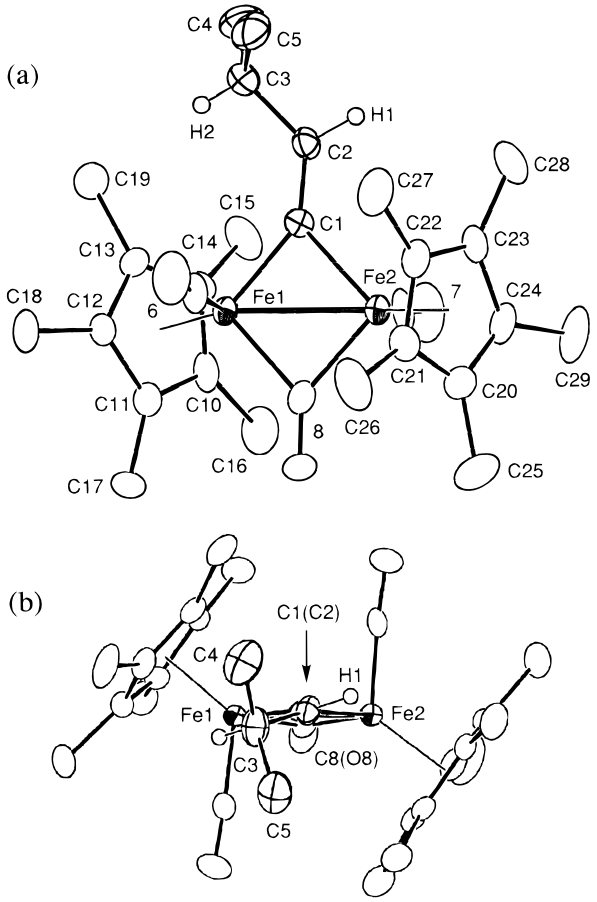

Figure 9. Molecular structure of **18e** drawn at the 30% probability level: (a) overview; (b) top view. (Numbers without atom names are for CO ligands.)

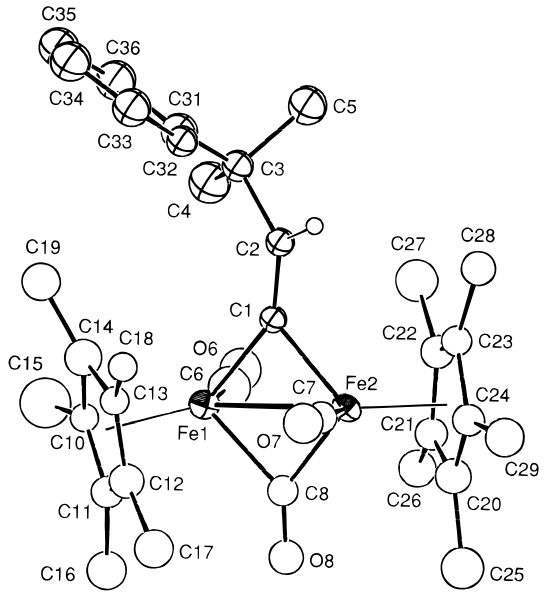

Figure 10. Molecular structure of **18h** drawn at the 30% probability level.

core (*cis* or *trans*) have been deduced. (1) When R = H and X ≃ Y (size), the *cis*- and *trans*-isomers are equilibrated in a solution. (2) When R = H and Me and X ≫ Y (size), the bigger substituent X occupies the space to which Cp(*) rings do not project and, consequently, the *cis*-isomer is formed as the major isomer. Complex **19a** falls into the latter category. In the case of Cp* complexes, a small difference in the size of X and Y leads to a *cis*-structure in order to minimize the steric repulsion between X and the bulky Cp* rings.

The situation of the vinylcarbyne complex **11** is rather complicated because the vinylcarbyne group can rotate around the $C_\alpha-C_\beta$ axis and yet the rotation is not completely free due to the conjugation of the allylic part. In addition, the β-carbon atom bearing the substituents is located not so close to the $Fe_2Cp^*_2$ core. Therefore, **11** may exist as an equilibrated mixture of the *trans*- and *cis*-isomers. Of the dinuclear complexes obtained by this study, only **11** gives the different X-ray and solution structures.[17]

Reaction of 3 with Nucleophiles. In contrast to the reaction with an electrophile, reaction of **3** with a nucleophile turned out to be sluggish; To our knowledge, no report on the nucleophilic addition to an **A**-type μ-allenylidene complex has appeared.

Sequential treatment of **3a** with $LiHBEt_3$ and MeOH afforded the μ-propenylidene complex **18b** (eq 12), which was also accessible via an addition reaction in the reverse order, as described above (eq 10). The reaction

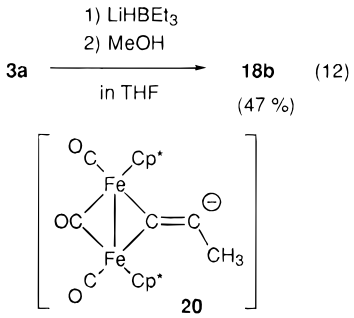

may be initiated by hydride addition to the γ-carbon atom to give the anionic intermediate **20**, protonation of which would lead to **18b**. Because attempted labeling experiments by using $LiDBEt_3$ and EtOD resulted in H−D scrambling, little information on the reaction sequence was obtained.

However, the regiochemistry of the nucleophilic addition has been confirmed by the structure of the reaction product of **3** with *n*-BuLi. Addition of *n*-BuLi to **3a**,**b** followed by MeOH quenching did not afford a product which incorporated a *n*-Bu group but rather a cyclic product **21** (eq 13), which was characterized spectroscopically. As a typical example, part of the ^{1}H-

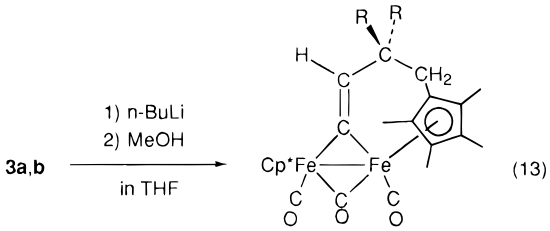

R= H (**21a**), Me (**21b**).

NMR spectrum of **21b** is reproduced in Figure 11. At first, the four methyl signals (3H × 4) observed separately indicated that one of the two Cp* ligands in **3** was functionalized, and the methylene protons of **3b** resulting from the functionalization were observed as two signals at δ_H 1.64 and 1.96 coupled with each other

Table 7. Selected Structural Parameters for the Core Part of μ-Vinylidene and μ-Allenylidene Complexes[a]

		vinylidene complex					allenylidene complex		
entry	substituents at β- and γ-terminus	**18l**[b] H, H	**18k** H, primary alkyl	**18e** H, secondary alkyl	**18h** H, tertiary alkyl	**4** acyl, acyl	**3a** H, H	**3b** Me, Me	**3c′** *n*-Bu, *n*-Bu
1	Fe1−C1	1.920(3)	1.931(7)	1.918(8)	1.97(3)	1.93(1)	1.946(5)	1.951(9)	1.94(2)
2	Fe2−C1	1.920(3)	1.922(7)	1.969(8)	1.94(2)	1.93(1)	1.937(5)	1.989(9)	1.93(2)
3	difference (1−2)	0	0.009	-0.051	0.03	0.00	0.009	0.038	0.01
4	Fe1−C1−C2	138.45(9)	141.8(6)	145.4(7)	146(2)	135(1)	136.8(4)	139.1(7)	138(1)
5	Fe2−C1−C2	138.45(9)	134.8(5)	131.8(6)	132(2)	142(1)	141.0(4)	139.8(7)	139(1)
6	difference (4−5)	0	7.0	13.6	14	7	4.2	0.7	1
7	C1−C2−C3	118(4)	130.1(8)	135(2)	129.1(7)	123(1)	178.1(7)	176(1)	172(1)
8	sum (4 + 7)	256	271.9	280	275	261[c]			
9	Fe2−Fe1−cp1[d]	140.4	140.8	138.1	138.8	141.3	139.9	140.1	140.0
10	Fe1−Fe2−cp2[d]	140.4	141.8	142.8	141.4	140.1	141.0	141.6	139.9
11	C1−Fe2−Fe1−cp1[d]	90.0	99.8	101.0	103.4	96.6	93.3	94.6	93.6
12	C1−Fe1−Fe2−cp2[d]	90.0	96.1	94.1	95.0	95.8	93.2	90.3	95.9
13	difference (11 − 12)	0	3.7	6.9	8.4	0.8	0.1	4.3	2.3
14	sum (11 + 12)	180.0	195.9	195.1	198.4	192.4	186.5	184.9	189.5
15	Fe1−C1−C2−C3	0	13(1)	11(2)	21(6)	28(2)			
16	Fe1−C1−C2−X[e]	0	15(4)	15(5)	32	31(1)			

[a] Interatomic distances in Å and bond angles in deg. [b] Imposed on a centrosymmetric site. [c] $^1/_2(4 + 5) + 7$. [d] cp1 and cp2 are centroids of the Cp* ligands, respectively. [e] X = H2 (**18k**,**l**), H1 (**18e**,**h**), C8 (**4**).

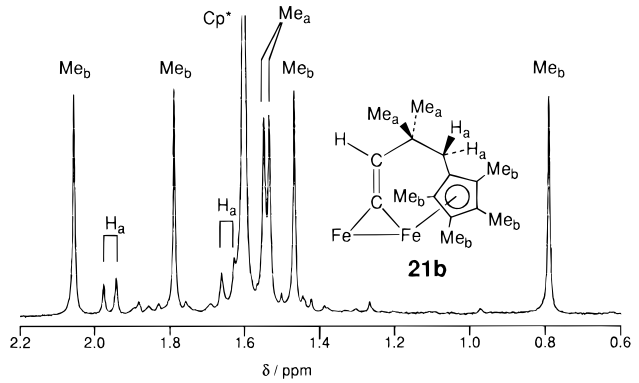

Figure 11. The alkyl region of the ^{1}H-NMR spectrum of **21b** (observed in $CDCl_3$ at 400 MHz).

Scheme 5

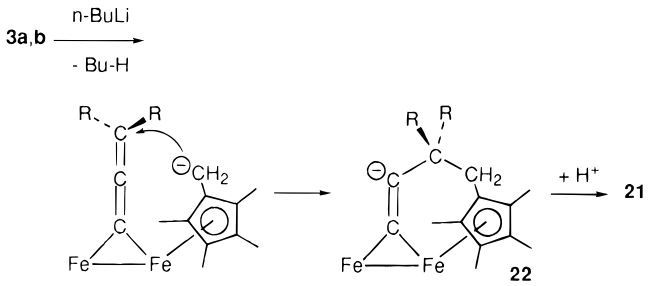

(d, J = 13.2 Hz), as confirmed by a decoupling experiment. In addition, the presence of a μ-C=CH moiety was suggested by the ^{13}C-NMR spectrum containing the characteristic deshielded quaternary carbon signal (δ_C 286.7) and a doublet signal (δ_C 131.0, J = 159 Hz). These spectral data led to the assignment as the cyclic structure **21**, which was also supported by the FD-MS spectrum (m/z = 532 (M^+)).

The formation of **21** can be readily explained in terms of the reaction sequence shown in Scheme 5: (i) deprotonation of a Cp* methyl group; (ii) nucleophilic addition to the γ-carbon atom giving the anionic intermediate **22**; (iii) protonation of **22**.

The structure of **21** clearly indicates that the nucleophile attacks the γ-carbon atom to form an anionic intermediate, with the β-carbon atom bearing the

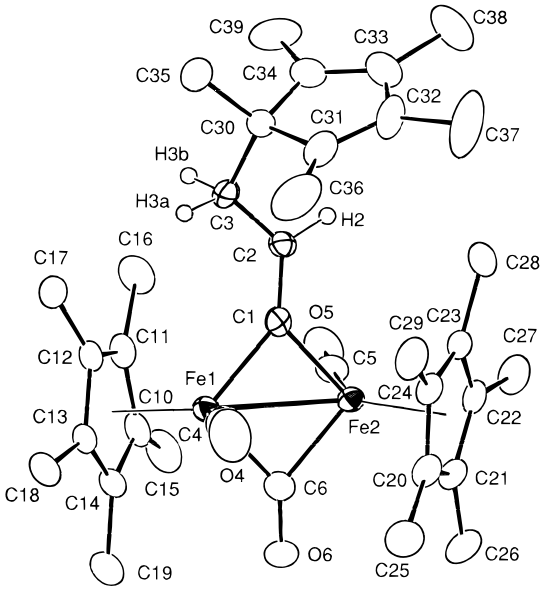

Figure 12. Molecular structure of **18k** drawn at the 30% probability level.

anionic charge. The regiochemistry is in sharp contrast to that observed for the electrophilic addition discussed above.

Attempted Synthesis of Allenylidene Cluster Compounds. The successful isolation of μ-allenylidene complexes **3** prompted us to convert them into cluster compounds by interaction with metal species. But attempted reactions of **3a**,**b** with various metal complexes resulted in recovery ($Pt(CH_2{=}CH_2)(PPh_3)_2$, $[RhCl(CH_2{=}CH_2)]_2$, $Cp^*_2Rh_2(CO)_2$, $Pd(PPh_3)_4$), decomposition of **3** ($Cp^*Rh(CO)_2$), or hydrogenation leading to **18a** ($Ru_3(CO)_{12}$). Only reaction with $Ru_3(CO)_{12}$ produced a new compound **18k**, which turned out to be a Cp*-substituted μ-vinylidene complex (eq 14), as characterized by X-ray crystallography (Figure 12 and Table 4). Complex **18k** was detected as the sole organometallic product by ^{1}H-NMR, and no Ru-incorporating product was isolated. The formation mechanism of **18k** is unknown at the present time.

Conclusion. The present study has established the first systematic synthetic method for **A**-type μ-alle-

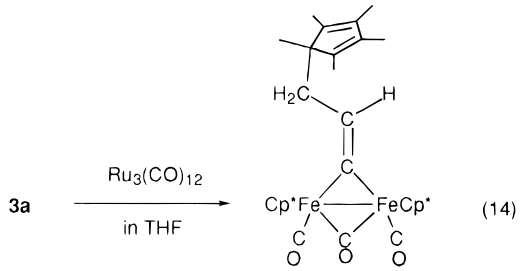

18k (50 %)

nylidene complexes **3** through nucleophilic addition to the diiron μ-ethynediyl complex **1**. The chemical reactivity of **3** is summarized in Scheme 6, as compared with that of the μ-vinylidene complex. The electrophile attacks the β-carbon atom to give the cationic vinylcarbyne species **11**, which is susceptible to subsequent nucleophilic addition to the γ-carbon atom to give a variety of μ-vinylidene complexes **18**. The regiochemistry is the same as that established for μ-vinylidene complexes. Thus, the three hydrocarbyl species **3**, **11**, and **18** can be interconverted by way of addition and elimination of H^+ and H^-. On the other hand, the nucleophile attacks the γ-carbon atom[19] to generate **20**, where anionic charge is localized on the β-carbon atom, to produce μ-vinylidene complexes **18** upon protonation. For μ-vinylidene complex, the reaction site of nucleophile has not been established because of its sluggishness toward such reagents.

A preliminary MO calculation[20] for the simplified model, $Cp_2Fe_2(\mu\text{-}C{=}C{=}CH_2)(\mu\text{-}CO)(CO)_2$, supports the experimental results. The second HOMO (**I**) of the allenylidene complex[21] bears the biggest filled p_y orbital at C_β, and the overall shape is similar to that of the corresponding orbital (**III**) of the vinylidene complex, $Cp_2Fe_2(\mu\text{-}C{=}CH_2)(\mu\text{-}CO)(CO)_2$. Therefore, the electrophile attacks the β-carbon atom in both cases. On the other hand, the LUMO (**II**) of the μ-allenylidene complex has the largest p-orbital coefficient at C_γ. In contrast, the μ-vinylidene complex does not have a ligand-based empty orbital of lower energy close to LUMO. Therefore, the nucleophile may attack the γ-carbon atom in allenylidene complexes, but vinylidene complexes are sluggish toward nucleophile.

Experimental Section

General Methods. All manipulations were carried out under an inert atmosphere by using standard Schlenk tube techniques. Ether, hexanes (Na−K alloy), and CH_2Cl_2 (P_2O_5) were treated with the appropriate drying agents, distilled, and stored under argon. The diiron μ-ethynediyl complex **1** was prepared by the method previously reported by us.[5b] Ethereal solutions of MeLi and PhLi were prepared from MeBr and PhBr, respectively. Other chemicals were purchased and used as received. Chromatography was performed on alumina (aluminum oxide, activity II−IV (Merck)) unless otherwise stated. ^{1}H- and ^{13}C-NMR spectra were recorded on JEOL EX-400 (^{1}H, 400 MHz; ^{13}C, 100 MHz) and Bruker AC200 spectrometers (^{1}H, 200 MHz). Solvents for NMR measurements containing 0.5% TMS were dried over molecular sieves, degassed, distilled under reduced pressure, and stored under Ar. IR and MS spectra were obtained on a JASCO FT/IR 5300 spectrometer and a Hitachi M-80 mass spectrometer, respectively. IR bands, unless otherwise stated, are for the CO stretching vibration (ν(C≡O)). Styryl ketones **13** were quantified by gas-liquid chromatography (GLC) (Silicon SE-30; Hitachi gas chromatograph 163 equipped with a FID detector).

Synthesis of Diiron Bridging Allenylidene Complexes 3 (One-Pot Synthesis). As a typical example, the synthetic procedure for the Me_2 derivative **3b** is described below. To a THF solution of **1** (252 mg, 0.48 mmol) cooled at −78 °C was added an ethereal MeLi solution (1.58 M, 0.46 mL, 0.73 mmol). After 10 min, the cooling bath was removed and the mixture was stirred at room temperature for 1 h. Then the mixture was cooled again, and the addition procedure was repeated (twice in this case) until **3b** became a major product, as judged by TLC (thin layer chromatography). The resulting mixture cooled at −78 °C was treated with MeOH (1 mL) and stirred for 5 min at the same temperature and 30 min at ambient temperature. After removal of the volatiles under reduced pressure, the products were extracted with ether and passed through an alumina plug. The filtrate was separated by column chromatography, and a blue-purple band eluted with CH_2Cl_2−hexanes = 1:4 was collected. Recrystallization from acetone gave **3b** as purple crystals (75 mg, 0.14 mmol, 29% yield). Anal. Calcd for $C_{28}H_{36}O_3Fe_2$: C, 63.18; H, 6.82. Found: C, 63.28; H, 6.78. The Bu derivative **3c** was prepared in an essentially similar manner, using *n*-BuLi. Anal. Calcd for $C_{34}H_{48}O_3Fe_2$: C, 66.29; H, 7.78. Found: C, 66.33; H, 7.92.

Synthesis of Diiron Bridging Allenylidene Complexes 3 (Two-Step Synthesis). As a typical procedure, the synthesis of **3a** from **1** via **2a** is described below. To a THF solution (12 mL) of **1** (490 mg, 0.95 mmol) was added a THF solution of $LiHBEt_3$ (1.0 M, 1.52 mL, 1.52 mmol). After 15 min, the mixture was warmed and stirred for 1 h at ambient temperature; the mixture was recooled at −78 °C, and MeOH (1 mL) was added. Then the mixture was stirred for 30 min at room temperature. After evaporation of the volatiles under reduced pressure, the products were extracted with Et_2O−hexanes = 1:3 and passed through a 15 cm alumina plug. After small amounts of Fp^*_2 and **1** were eluted with Et_2O−hexanes = 1:3, **2a** (purple band) was eluted with Et_2O and then with THF. Concentration and addition of hexanes followed by cooling at −20 °C gave **2a** (348 mg, 0.67 mmol, 71% yield) as a purple powder. **2a**: ^{1}H NMR ($CDCl_3$) δ 9.57 (1H, d, J = 8.9 Hz), 8.11 (1H, d, J = 8.9 Hz), 1.67, 1.62 (15H × 2, s × 2, Cp^*_2). ^{13}C NMR ($CDCl_3$): δ 9.4, 8.8 (q × 2, J = 128 Hz), 99.5, 99.7 (s × 2, C_5Me_5), 141.8 (d, J = 152 Hz, =CH), 190.2 (d, J = 168 Hz, CHO), 213.1, 213.7 (s × 2, CO), 272.3 (s, μ-CO), 350.0 (s, Fe_2C=). Anal. Calcd for $C_{26}H_{32}O_3Fe_2$: C, 60.06; H, 6.15. Found: C, 60.01; H, 6.21.

To a THF solution (10 mL) of **2a** (350 mg, 0.68 mmol) cooled at −78 °C was added a THF solution of $LiHBEt_3$ (1.0 M, 0.95 mL, 0.95 mmol). After 10 min, the mixture was warmed and stirred for 1 h at ambient temperature. Then the resulting mixture was cooled at −78 °C, and MeOH (1.5 mL) was added. After evaporation of the volatiles under reduced pressure, the products were extracted with THF and passed through an alumina plug. Concentration and cooling of the filtrate and crystallization from acetone gave **3a** (184 mg, 0.37 mmol, 54% yield) as a purple crystals. **3a**: Anal. Calcd for $C_{26}H_{32}O_3Fe_2$ C, 61.96; H, 6.35. Found: C, 61.68; H, 6.55.

Unsymmetrically substituted μ-allenylidene complexes **3d**−**h** were prepared by the method described for **3a** by using the appropriate combination of **2** and RLi. **3d**: Anal. Calcd for $C_{32}H_{36}O_3Fe_2$ C, 66.26; H, 6.21. Found: C, 65.82; H, 5.76. **3e**: Anal. Calcd for $C_{30}H_{40}O_3Fe_2$ C, 64.34; H, 7.14. Found: C,

(19) It was reported that nucleophilic addition to **B**-type complexes led to an anionic acetylide species where the anionic charge was localized on the metal center.[4]

(20) Preliminary EHMO calculations were carried out by using a program obtained from Nishimoto, K.; Imamura, I.; Yamaguchi, K.; Yamabe, S.; Kitaura, K. *Bunshisekkei-no-tame-no-ryoshirikigaku* (*Quantum Chemistry for Molecular Design*); Kodansha: Tokyo, 1989.

(21) The HOMO was a metal-based orbital with the total energy very similar to I within the accuracy of the EHMO calculation.

Scheme 6

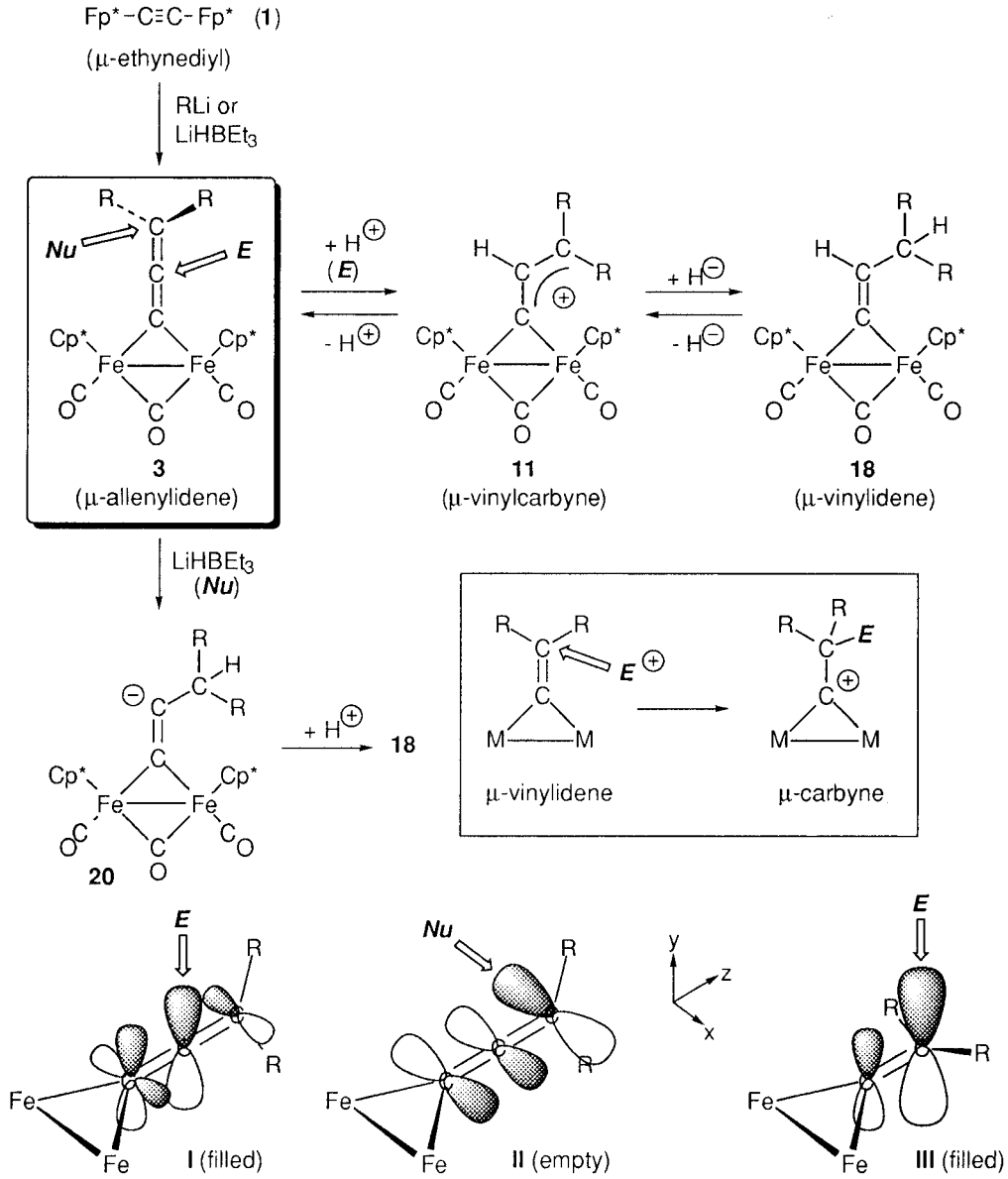

64.05; H, 6.92. **3f**: Anal. Calcd for $C_{33}H_{38}O_3Fe_2$ C, 66.72; H, 6.46. Found: C, 67.09; H, 6.50. **3g**: Anal. Calcd for $C_{31}H_{38}O_3Fe_2$ C, 64.83; H, 7.37. Found: C, 64.96; H, 7.32. **3h**: Anal. Calcd for $C_{31}H_{42}O_3Fe_2$ C, 64.83; H, 7.37. Found: C, 64.05; H, 7.98.

Synthesis of 3c′. The ethynediyl complex (μ-C≡C)[Fe(η^5-C_5Me_4Et)$(CO)_2]_2$ (**1′**) was prepared in essentially the same method as that described for the Cp* derivative **1**.[5b] **1′** (brick-red crystals, 75% yield): ^{1}H NMR ($CDCl_3$) δ 1.01 (6H, t, J = 7.7 Hz, CH_2CH_3 × 2), 1.81 (24H, s, C_5Me_4Et), 2.26 (4H, q, J = 7.7 Hz, CH_2CH_3 × 2). IR: (KBr) 1992, 1942 cm^{-1}. Anal. Calcd for $C_{28}H_{34}O_3Fe_2$: C, 61.59; H, 6.23. Found: C, 61.68; H, 6.02.

Complex **3c′** was prepared by treatment of **1′** with *n*-BuLi in 36% yield according to the one-pot synthesis method. ^{1}H NMR ($CDCl_3$): δ 0.94 (6H, t, J = 7.3 Hz, $C_5Me_4CH_2CH_3$), 1.01 (6H, t, J = 7.3 Hz, CH_3, $CH_2CH_2CH_2CH_3$), ~1.44 (m, $CH_2CH_2CH_2CH_3$), 1.52, 1.54, 1.66, 1.71 (3H × 4, C_5Me_4Et), ~1.65 (m, $CH_2CH_2CH_2CH_3$), 2.17 (4H, q, J = 7.3 Hz, $C_5Me_4CH_2CH_3$), 2.27, 2.33 (1H × 2, m, $CH_2CH_2CH_2CH_3$). ^{13}C NMR ($CDCl_3$): δ 8.5, 8.6, 8.7 (q, J = 127 Hz, C_5Me_4Et), 13.9 (q, J = 125 Hz, $C_5Me_4CH_2CH_3$), 14.1 (q, J = 125 Hz, $CH_2CH_2CH_2CH_3$), 17.5 (t, J = 129 Hz, $C_5Me_4CH_2CH_3$), 22.9 (t, J = 129 Hz, $CH_2CH_2CH_2CH_3$), 31.3 (t, J = 127 Hz, $CH_2CH_2CH_2CH_3$), 37.7 (t, J = 127 Hz, $CH_2CH_2CH_2CH_3$), 96.3, 97.0, 98.5, 98.6, 102.6 (s × 5, C_5Me_4Et), 111.1 (s, C_γ), 191.8 (s, C_α), 205.6 (s, C_β), 214.1 (s, Fe−CO), 280.8 (s, μ-CO). IR: (KBr) 1916, 1769 cm^{-1}.

Formation of Alkenylvinylidene Complex 5. To a THF (4 mL) solution of **2a** (149 mg, 0.29 mmol) cooled at −78 °C was added an ethereal solution of MeLi (1.4 M, 0.27 mL, 0.38 mmol). After the reaction mixture was stirred for 10 min at the same temperature, stirring was continued for 1 h at ambient temperature. Then the mixture was cooled at −78 °C, and MeOH (1 mL) was added. Extraction with Et_2O−hexanes = 1:3 to 1:2 followed by filtration through an alumina plug gave a purple solution, from which **5a** (112 mg, 2.22 mmol, 75% yield) was isolated as black-purple crystals. **5a**: ^{1}H NMR (C_6D_6) δ 1.52, 1.60 (15H × 2, s × 2, Cp^*_2), 4.94 (1H, dd, J = 10 and 2 Hz, CH=CH_2), 5.30 (1H, dd, J = 17 and 2 Hz, CH=CH_2), 7.26 (1H, ddd, J = 17, 10, and 2 Hz, CH=CH_2), 8.32 (1H, d, J = 10 Hz, CH−CH=CH_2). ^{13}C NMR (C_6D_6): δ 8.9, 9.8 (q × 2, J = 128 Hz, C_5Me_5), 98.7, 98.9 (s × 2, C_5Me_5), 104.2 (t, J = 157 Hz, =CH_2), 138.2 (d, J = 147 Hz, CH=CH_2), 140.1 (d, J = 151 Hz, CH-CH=CH_2), 215.1, 215.2 (s × 2, CO), 276.1 (s, μ-CO), 305.6 (Fe_2C). IR: (KBr) 1926, 1776 (ν(C≡O)) cm^{-1}; (CH_2Cl_2) 1921, 1770 cm^{-1}. Anal. Calcd for $C_{27}H_{34}O_3Fe_2$: C, 62.60; H, 6.56. Found: C, 62.29; H, 6.67.

A similar reaction of **2a** (110 mg, 0.21 mmol) with *n*-BuLi (1.62 M, 0.2 mL, 0.32 mmol) gave **5b** (76 mg, 0.14 mmol, 67% yield). A mixture of *cis*- and *trans*-**5b**: ^{1}H NMR (C_6D_6)

δ 1.07, 1.16 (3H, t, J = 7.3 Hz, CH_3), 1.54, 1.56, 1.62, 1.65 (s × 4, Cp*$_2$), 1.74 (2H, m, CH_2CH$_3$; the signal for the other isomer was overlapped with the Cp* signal), 2.42, 2.68 (2H, m, CH_2CH$_2$CH$_3$), 5.23, 5.70 (1H, dt, J = 15 and 7 Hz, =CH−Pr), 6.94, 6.97 (1H, dd, J = 11 and 5 Hz, CH=CH−Pr), 8.28, 8.54 (1H, d, J = 10 Hz, =CH−CH=CH). ^{13}C NMR (C_6D_6): δ 8.9, 9.8 (q × 2, J = 128 Hz, C$_5$*Me*$_5$), 14.1, 14.4 (q × 2, J = 128 Hz, CH_3), 24.1 (t, J = 126 Hz, CH_2CH$_3$), 30.8, 35.5 (t, J = 126 Hz, CH_2CH$_2$CH$_3$), 98.6, 98.7, 98.8 (s, C_5Me$_5$), 119.3, 121.2 (d, J = 150 Hz, =CH−CH=CH−), 131.9, 133.1 (dt, J = 151 and 5 Hz, =CH−Pr), 133.8, 137.0 (dd, J = 149 and 7 Hz, Fe$_2$C=CH), 215.2, 215.3 (s, CO), 276.5, 276.6 (s, μ-CO), 301.6, 306.7 (s, Fe$_2$C). IR: (KBr) 1921, 1773 cm^{-1}. Anal. Calcd for $C_{30}H_{40}O_3Fe_2$: C, 64.34; H, 7.14. Found: C, 64.69; H, 7.30.

Reaction of Phenylacetylide Complex 12 with RLi (Formation of Styryl Ketone 13). As a typical example, the reaction of **12a** with *t*-BuLi is described below. To a stirred THF solution (20 mL) of **12a** (506 mg, 1.82 mmol) cooled at −78 °C was added *t*-BuLi (1.25 M hexane solution, 1.75 mL, 2.18 mmol). Because TLC of the reaction mixture after 1 h revealed the presence of a small amount of unreacted **12a**, 1 mL of *t*-BuLi (1.25 mmol) was added. After 30 min, MeOH (2 mL) was added and the residue was subjected to column chromatography (eluted with CH_2Cl_2/hexanes = 1:15 to 1:5). Further separation by preparative TLC (on silica gel eluted with CH_2Cl_2/hexanes = 1:1; Kieselgel 60 PF_{254} (Merck)) gave **13c** (213 mg, 1.13 mmol, 62%) as colorless crystals, together with unidentified pale yellow product (36 mg). *trans*-**13c**: ^{1}H NMR ($CDCl_3$) δ 1.23 (9H, s, *t*-Bu), 7.13 (d, J = 16 Hz, =C(H)-CO), 7.37−7.38 (3H, m, Ph), 7.56−7.58 (2H, m, Ph), 7.69 (1H, J = 16 Hz, Ph−CH=). ^{13}C NMR ($CDCl_3$): δ 26.3 (q, 127, C*Me*$_3$), 43.2 (s, *C*Me$_3$), 120.1 (d, 155 Hz, =*C*H−CO), 128.2 (dt, J = 155 and 5 Hz, *m*-Ph), 128.8 (dd, J = 154 and 6 Hz, *o*-Ph), 130.1 (dt, J = 158 and 7 Hz, *p*-Ph), 134.9 (t, J = 6 Hz, *ipso*-Ph), 142.8 (dt, J = 154 and 5 Hz, Ph−*C*H=), 204.2 (s, C=O). IR: (KBr) 1682 (ν(C=O)), 1614, 1576 (ν(C=C)) cm^{-1}.

The reaction of **12a** and *n*-BuLi gave a mixture of *cis*- and *trans*-**13b** (54% yield). **13b**:^{1}H NMR ($CDCl_3$) δ 0.73 (3H, t, J = 7.3 Hz, CH_3), 1.19−1.27, 2.77−2.89, 3.24−3.38 (2H × 3, m, CH_2CH_2CH_2CH$_3$), 7.12−7.30 (m, 7H, Ph−C(H)=C(H)). IR: (KBr) 1720, 1700, 1602 cm^{-1}. A small amount of an organometallic product assignable to Cp$_2$Fe$_2$(CO)$_2$(μ-CO)-(μ-C=CHPh) (41 mg, 0.15 mmol, 7% yield) was also isolated. ^{1}H NMR ($CDCl_3$): δ 4.70, 4.81 (5H × 2, s, Cp$_2$), 7.30 (m, 5H, Ph), 8.55 (1H, s, =CH). ^{13}C NMR ($CDCl_3$): δ 90.1, 90.7 (d × 2, J = 180 Hz, Cp$_2$), 124.7 (d, J = 159 Hz, Ph), 126.5 (d, J = 159 Hz, Ph), 128.2 (d, J = 156 Hz, Ph), 140.9 (s, *ipso*-Ph), 143.0 (d, J = 156 Hz, =CH), 211.7, 211.9 (s × 2, CO), 271.3 (s, μ-CO), 279.7 (s, Fe$_2$C). IR: (KBr) 2000, 1951, 1794 cm^{-1}. Anal. Calcd for $C_{21}H_{16}O_3Fe_2$: C, 58.94; H, 3.74. Found: C, 58.76; H, 3.66.

The GLC yield of styryl ketone (eq 4) was determined as follows. To a THF solution (4 mL) of **12** (ca. 0.25 mmol) cooled at −78 °C was added RLi (1.2−2.9 equiv) until **12** was consumed, as judged by TLC analysis. After 1 h, the resulting mixture was hydrolyzed with MeOH (1 mL). Then an internal standard (**12a**, *n*-$C_{14}H_{30}$; **12b**, *n*-$C_{16}H_{34}$; **12c**, phenanthrene) was added, and the yields of products were determined by GLC analysis. An authentic sample of **12a** was purchased.

Reaction of Phenylacetylide Complex 12 with *n*-BuLi in the Presence of PPh$_3$. To a mixture of **12a** (313 mg, 1.33 mmol) and PPh_3 (589 mg, 2.25 mmol) dissolved in THF (12 mL) was added *n*-BuLi (1.63 M hexane solution, 0.9 mL, 1.46 mmol) at −78 °C. After 1 h, MeOH was added to destroy the remaining *n*-BuLi. After removal of the volatiles, the products were extracted with ether, passed through an alumina plug,and then subjected to chromatographic separation (eluted with CH_2Cl_2−hexane = 1:3). **15a** was isolated from an orange band. **15a** (brick red crystals, 519 mg, 0.87 mmol, 65% yield): ^{1}H NMR ($CDCl_3$) δ 0.74 (3H, t, J = 7.3 Hz, CH_3), 0.95, 1.06, 1.21 (2H × 3, m, CH_2CH_2CH_2CH$_3$), 4.59 (5H, s, Cp), 7.20−7.34 (5H, m, Ph). ^{13}C NMR ($CDCl_3$): δ 14.0 (q, J = 123 Hz, CH_3), 22.4, 26.5, 40.9 (t × 3, J = 123Hz, CH_2CH_2CH_2CH_3), 84.6 (d, J = 178 Hz, Cp), 125.7 (d, J = 160 Hz, Ph), 127.0 (d, J = 160 Hz, Ph), 128.1 (dd, J_{CH} = 160 Hz, J_{CP} = 9 Hz, PPh), 129.6 (dd, J_{CH} = 160 Hz, J_{CP} = 28 Hz, PPh), 133.3 (d, J = 162 Hz, Ph), 144.2 (s, Ph), 141.6 (d, J = 151 Hz, =CH), 165.2 (d, J_{CP} = 22 Hz, Fe−C=), 216.5 (s, Fe−CO), 220.8 (s, Bu−*C*=O). IR (KBr) 1932 (ν(C≡O)), 1647 (ν(C=O)) cm^{-1}. Anal. Calcd for $C_{37}H_{35}O_2PFe$: C, 74.29; H, 5.86. Found: C, 73.96; H, 5.90.

The reaction of **12b** (273 mg, 0.78 mmol) with *n*-BuLi (1.01 mmol) in the presence of PPh_3 (411 mg, 1.57 mmol) afforded **15b** (284 mg, 0.42 mmol) as orange crystals after crystallization from toluene−MeOH. **15b**: ^{1}H NMR ($CDCl_3$) δ 0.61 (3H, t, CH_3), 0.86, 1.21, 1.23 (2H × 3, m, CH_2CH_2CH_2CH$_3$), 1.56 (15H, s, Cp*), 6.46 (1H, s, =CH), 6.88−7.51 (5H, m, Ph). ^{13}C NMR ($CDCl_3$): δ 9.9 (q, J = 127 Hz, C$_5$*Me*$_5$), 13.9 (q, J = 127 Hz, $CH_2CH_2CH_2CH_3$), 22.1 (t, J = 126 Hz, $CH_2CH_2CH_2CH_3$), 25.6 (t, J = 126 Hz, $CH_2CH_2CH_2CH_3$), 38.9 (t, J = 125 Hz, $CH_2CH_2CH_2CH_3$), 93.5 (s, C_5Me$_5$), 124.6 (d, J = 162 Hz, Ph), 126.4 (d, J = 154 Hz, Ph), 127.6 (dd, J_{CH} = 160 Hz and J_{CP} = 9 Hz, Ph), 127.9 (dd, J = 158 and 9 Hz, Ph), 129.5 (d, J = 158 Hz, Ph), 140.6 (s, Ph), 134.2 (d, J = 156 Hz, =CH), 171.6 (d, J = 18 Hz, FeC=), 217.7 (s, Fe−CO), 223.8 (s, *C*O−Bu). IR: (KBr) 1932, 1647 cm^{-1}. Anal. Calcd for $C_{42}H_{45}O_2PFe$: C, 75.48; H, 6.73. Found: C, 75.42; H, 6.98.

Protonation of 3 Leading to Cationic Vinylcarbyne Complex 11. To a THF solution (10 mL) of **3c** (121 mg, 0.21 mmol) cooled at 0 °C was added CF_3SO_3H (20 μL, 0.23 mmol). While the mixture was gradually warmed to room temperature, the solution color changed from green to dark brown and **11c** was precipitated. Removal of the supernatant solution via a cannula and drying under reduced pressure gave **11c**(CF_3SO_3 salt)·THF as a dark brown powder (104 mg, 0.13 mmol, 62% yield). **11c** (*cis*-isomer: isolated sample containing a THF solvate): ^{1}H NMR (CD_2Cl_2) δ 1.16 (4H, m, THF), 1.73 (30H, s, Cp*$_2$), 3.67 (4H, m, THF), 6.95 (1H, d, J = 15.6 Hz, =CHPh), 7.59−7.65 (3H, m, *m*- and *p*-Ph), 7.97 (2H, d, J = 6.8 Hz, *o*-Ph), 9.31 (1H, d, J = 15.6 Hz, Fe$_2$C=CH). ^{13}C NMR (CD_2Cl_2): δ 9.3 (q, J = 127 Hz, C$_5$*Me*$_5$), 26.1 (t, J = 132 Hz, THF), 68.2 (t, J = 143 Hz, THF), 104.1 (s, C_5Me$_5$), 130.2 (dd, J = 158 and 7 Hz, *m*-Ph), 130.6 (dd, J = 162 and 7 Hz, *o*-Ph), 132.5 (dt, 155 and 7 Hz, *p*-Ph), 134.3 (t, J = 7 Hz, *ipso*-Ph), 134.6 (d, J = 155 Hz, *C*HPh), 149.3 (d, J = 158 Hz, C−*C*H), 210.6 (s, CO), 259.4 (s, μ-CO), 452.0 (s, Fe$_2$C). IR: (KBr) 1976, 1816, (ν(C≡O)) 1553 (ν(C=C)) cm^{-1}; (CH_2Cl_2) 1982, 1831 (ν-(C≡O)) cm^{-1}. Anal. Calcd for $C_{37}H_{45}O_7F_3SFe_2$ (**11c**·OTf·-THF): C, 55.38; H, 5.65. Found: C, 54.92; H, 5.24. **11c** (*trans*-isomer detected by ^{1}H-NMR experiment): ^{1}H NMR (CD_2Cl_2) δ 1.61, 1.77 (15H × 2, s × 2, Cp*$_2$), 7.11 (1H, d, J = 12.7 Hz, =CHPh), 7.39 (2H, d, J = 7.3 Hz, *o*-Ph), 7.25−7.35 (3H, m, *m*- and *p*-Ph), 8.00 (1H, d, J = 12.7 Hz, Fe$_2$C=CH).

The BF_4 salt was obtained by a similar procedure, using HBF_4·OEt_2 in place of CF_3SO_3H. ^{1}H NMR ($CDCl_3$): δ 1.75 (30H, s, Cp*$_2$), 6.95 (1H, d, J = 14.5 Hz, =CHPh), 8.00−8.15 (3H, m, *m*- and *p*-Ph), 8.55−8.70 (2H, m, *o*-Ph), 9.55 (1H, d, J = 14.5 Hz, Fe$_2$C=CH). IR: (KBr) 1967, 1812 (ν(C≡O)), 1551 (ν(C=C)) cm^{-1}. Anal. Calcd for $C_{33}H_{39}O_3BF_4$-Cl_2Fe_2 (**11c**·BF_4·CH_2Cl_2): C, 52.63; H, 5.22. Found: C, 53.34; H, 5.29.

Similar reaction of **3a**,**b** with CF_3SO_3H afforded **11a** and **11b**, respectively, which were characterized on the basis of the spectroscopic data as discussed in the text. **11a**: ^{1}H NMR (CD_2Cl_2) δ 1.65 (30H, s, Cp*$_2$), 5.48 (1H, dd, J = 16.9 and 1.2 Hz, *trans*-CH_2), 6.21 (1H, dd, J = 11.3 and 1.2 Hz, *cis*-CH_2), 8.58 (1H, dd, 16.9 and 11.3 Hz, CH). ^{13}C NMR (CD_2Cl_2): δ 9.4 (q, J = 129 Hz, C$_5$*Me*$_5$), 105.3 (s, C_5Me$_5$), 211.3 (s, CO),

262.2 (s, μ-CO), 500.9 (d, J = 7 Hz, Fe_2C).[14] IR: (CH_2Cl_2) 1979, 1832 (ν(C≡O)) cm^{-1}. IR: (CH_2Cl_2) 1985, 1838 (ν(C≡O)) cm^{-1}. **11b**: ^{1}H NMR (CD_2Cl_2) δ 1.71 (30H, s, Cp*$_2$), 2.02, 2.31 (3H × 2, s × 2, Me_2), 8.32 (1H, s, CH). ^{13}C NMR (CD_2Cl_2): δ 9.0 (q, J = 129 Hz, C_5Me_5), 22.9, 27.8 (q × 2, J = 129 Hz, CMe_2), 104.1 (s, C_5Me_5), 143.6 (s, CMe_2), 152.6 (d, J = 155 Hz, CH), 210.1, 212.6 (s × 2, CO), 260.7 (s, μ-CO), 455.9 (s, Fe_2C). IR: (CH_2Cl_2) 1979, 1832 cm^{-1}; (KBr) 1985, 1838 cm^{-1}.

Reaction of 11 with Et_4NBH_4 Giving Vinylidene Complexes 18a,e. To a CH_2Cl_2 solution of **3a** (199 mg, 0.40 mmol) cooled at 0 °C was added CF_3SO_3H (42 μL). After the mixture was gradually warmed to room temperature, Et_4NBH_4 (201 mg, 1.38 mmol) was added to the resulting mixture. After the mixture was stirred for several minutes, the volatiles were removed under reduced pressure and the residue was subjected to chromatographic separation. Elution with hexanes gave a purple band, from which **18a** (84 mg, 0.17 mmol, 41% yield) was isolated as a purple powder. **18a**: Anal. Calcd for $C_{26}H_{34}O_3Fe_2$ C, 61.69; H, 6.77. Found: C, 61.14; H, 6.77.

Prolonged stirring (overnight) after the addition of Et_4NBH_4 afforded the μ-propylidene complex **19a**, a reduced product. **19a** (purple-red crystals): ^{1}H NMR ($CDCl_3$) δ 1.57 (3H, t, J = 7.4 Hz, CH_3), 1.70 (30H, s, Cp*$_2$), 3.46 (quint, J = 7.4 Hz, CH_2), 9.78 (1H, t, J = 7.4 Hz, μ-CH). ^{13}C NMR ($CDCl_3$): δ 10.0 (q, J = 127 Hz, C_5Me_5), 20.5 (q, J = 125 Hz, CH_3), 50.9 (t, J = 126 Hz, CH_2), 96.1 (s, C_5Me_5), 201.0 (d, J = 128 Hz, μ-CH), 214.4 (s, CO), 278.9 (μ-CO). Anal. Calcd for $C_{26}H_{36}O_3Fe_2$: C, 61.44; H, 7.14. Found: C, 61.38; H, 7.14.

The Me_2 derivative **18e** was prepared in essentially the same manner as that described above, starting from **3b**. Anal. Calcd for $C_{28}H_{38}O_3Fe_2$: C, 62.94; H, 7.17. Found: C, 62.68; H, 7.07.

Reaction of the parent allenylidene complex **3a** for a long period (overnight) afforded a mixture of the μ-propenylidene complex **18a** and the μ-phenylpropylidene complex **19a** (18%), which were separated by column chromatography.

The reaction of the Ph−allenylidene complex **3c** afforded the μ-phenylpropylidene complex **19b** (20%) as the sole isolable organometallic product. **19b**: ^{1}H NMR ($CDCl_3$) δ 1.72 (30H, s, Cp*$_2$), 3.28, 3.64 (2H × 2, m × 2, $PhCH_2CH_2$), 7.30−7.37 (5H, m, Ph), 9.82 (1H, t, J = 7.6 Hz, μ-CH). ^{13}C NMR ($CDCl_3$): δ 10.0 (q, J = 127 Hz, C_5Me_5), 43.0, 60.9 (t × 2, J = 127 Hz, $PhCH_2CH_2$), 96.2 (s, C_5Me_5), 125.5 (dd, J = 159 and 7 Hz, *p*-Ph), 128.4 (dd, J = 159 and 7 Hz, *o*-Ph), 128.5 (dd, J = 153 and 7 Hz, *m*-Ph), 143.6 (s, *ipso*-Ph), 196.4 (d, J = 129 Hz, μ-CH), 214.2 (s, CO), 278.4 (μ-CO). FD-MS: m/z 584 (M^+). Anal. Calcd for $C_{32}H_{40}O_3Fe_2$: C, 65.77; H, 6.90. Found: C, 65.56; H, 6.87.

Reaction of 11 with $LiCuR_2$ Giving Functionalized Vinylidene Complexes 18. As a typical example, the synthetic procedure for **18f** is described in detail. To an ethereal solution (25 mL) of **3b** (187 mg, 0.35 mmol) cooled at 0 °C was added CF_3SO_3H (37 μL, 0.42 mmol). Then an ethereal solution of $LiCuMe_2$ (prepared from CuI (334 mg, 1.75 mmol) and MeLi (1.1 M, 3.2 mL, 3.51 mmol) in Et_2O (7 mL)) was added to the resulting solution of **11b**. After the mixture was gradually warmed to ambient temperature with stirring (1 h), the volatiles were removed under reduced pressure. Extraction with CH_2Cl_2 and filtration through an alumina plug followed by separation by column chromatography gave a purple band (eluted with hexanes), from which **18f** was isolated as a purple powder (54 mg, 0.10 mmol, 23% yield). **18f**: Anal. Calcd for $C_{29}H_{40}O_3Fe_2$ C, 63.52; H, 7.35. Found: C, 63.39; H, 7.27.

Other reactions were carried out in essentially the same manner using the appropriate μ-allenylidene complexes and $LiCuR_2$. The reaction of **11c** with $LiCuPh_2$ gave **18i** (27% yield) along with the deprotonated product **3c** (26% yield). **18b**: FD-MS m/z 520 (M^+). Anal. Calcd for $C_{27}H_{38}O_4Fe_2$ (**18b**·H_2O): C, 60.25; H, 7.12. Found: C, 59.80; H, 6.89. **18c**: FD-MS m/z 562 (M^+). **18e**: Anal. Calcd for $C_{28}H_{38}O_3Fe_2$ C, 62.94; H, 7.17. Found: C, 62.78; H, 7.27. **18f**: FD-MS m/z 548 (M^+). Anal. Calcd for $C_{29}H_{40}O_3Fe_2$: C, 63.52; H, 7.35. Found: C, 63.39; H, 7.27. **18g**: FD-MS m/z 590 (M^+). **18h**: Anal. Calcd for $C_{34}H_{42}O_3Fe_2$ C, 66.27; H, 6.79. Found: C, 66.22; H, 6.73. **18i**: Anal. Calcd for $C_{38}H_{42}O_3Fe_2$ C, 69.32; H, 6.43. Found: C, 68.52; H, 6.43. Analytically pure samples of **18c**,**g** were not obtained despite of several attempts, and **18d** was obtained as an inseparable mixture with Fp*$_2$.

Reaction of 11a with $HNEt_2$ Giving Aminovinylidene Complex 18j. To an acetone (15 mL) solution of **3a** (254 mg, 0.50 mmol) cooled at 0 °C was added CF_3SO_3H (60 μL, 0.68 mmol) via a microsyringe. After the mixture was gradually warmed up to room temperature, $HNEt_2$ (0.5 mL, 4.83 mmol) was added to the resulting mixture. After 5 min, the volatiles were evaporated and the residue was subjected to column chromatography. Elution with Et_2O:hexanes 1:3 to 1:1 gave a mixture of byproducts, such as Fp*$_2$, and then a purple band was eluted with Et_2O. **18j** was isolated as a purple powder (90 mg, 0.16 mmol, 31% yield). An analytically pure sample of **18j** was not obtained despite of several attempts. FD-MS: m/z 577 (M^+).

Transformation of 3a into 18a via $LiHBEt_3$ Treatment. To a THF solution (20 mL) of **3a** (92 mg, 0.18 mmol) cooled at −78 °C was added $LiHBEt_3$ (1.0 M THF solution, 2.74 mL, 2.74 mmol). The mixture was gradually warmed to ambient temperature, and the mixture continued to stir for 10 min. Then MeOH (1 mL) was added. After removal of the volatiles under reduced pressure, the residue was extracted with CH_2Cl_2 and passed through an alumina plug. Crystallization from CH_2Cl_2−hexanes gave 55 mg of purple solid, which consisted of a 1:4 mixture of **18a** (47%) and recovered **3a** (12%), as revealed by ^{1}H-NMR analysis.

Reaction of 3 with *n*-BuLi Giving Cyclic Product 21. To a THF solution (20 mL) of **3a** (165 mg, 0.33 mmol) cooled at −78 °C was added *n*-BuLi (1.6 M hexane solution, 1.40 mL, 2.27 mmol). While the mixture was gradually warmed to room temperature with stirring, the solution color changed from purple to dark brown. After 1 h, the mixture was cooled again to −78 °C and hydrolyzed with MeOH (4 mL). The solution color changed to purple-red. Removal of the inorganic salts by filtration through an alumina plug followed by chromatographic separation (eluted with hexanes−Et_2O 10:1) gave a purple-red band, from which **21a** was isolated as a purple-red powder (85 mg, 0.17 mmol, 52% yield). **21a**: ^{1}H NMR (C_6D_6) δ 0.95, 1.53, 1.73, 2.02 (3H × 4, s, η^5-$C_5Me_4CH_2$), 1.61 (15H, s, Cp*), 1.52 (1H, m, η^5-$C_5Me_4CH_2$), 2.16 (1H, ddd, J = 13.1, 5.3, and 2.0 Hz, η^5-$C_5Me_4CH_2$), 2.95 (1H, m, =CCH_2), 3.27 (1H, m, =CCH_2), 6.94 (1H, dd, J = 7.3 and 4.4 Hz, =CH). ^{13}C NMR ($CDCl_3$): δ 8.9 (q, J = 128 Hz, C_5Me_5), 8.2, 8.4, 8.6, 9.2 (q × 4, J = 128 Hz, η^5-$C_5Me_4CH_2$), 21.0 (t, J = 128 Hz, η^5-$C_5Me_4CH_2$), 42.8 (t, J = 125 Hz, =$CHCH_2$), 97.3 (s, C_5Me_5), 90.3, 97.8, 100.1, 103.0, 106.5 (s × 5, η^5-$C_5Me_4CH_2$), 118.5 (d, J = 160 Hz, =CH), 214.4, 214.9 (s, Fe-CO), 281.3 (s, μ-CO), 290.6 (s, μ-C=C). IR: (CH_2Cl_2) 1918, 1766 cm^{-1}. FD-MS: m/z 504 (M^+). Anal. Calcd for $C_{26}H_{34}O_4Fe_2$ (**21a**·H_2O): C, 60.20; H, 6.47. Found: C, 60.58; H, 6.46.

A similar reaction of **3b** with *n*-BuLi gave **21b** in 24% yield. ^{1}H NMR (C_6D_6): δ 0.79, 1.46, 1.78, 2.05 (3H × 4, s, η^5-$C_5Me_4CH_2$), 1.60 (15H, s, Cp*), 1.53, 1.54 (3H × 2, s × 2, CMe_2), 1.64, 1.96 (1H × 2, d × 2, J = 13.7 Hz, η^5-$C_5Me_4CH_2$), 6.71 (1H, s, =CH). ^{13}C NMR ($CDCl_3$): δ 9.0 (q, J = 127 Hz, C_5Me_5), 8.6, 8.7, 9.3, 10.5 (q × 4, J = 127 Hz, η^5-$C_5Me_4CH_2$), 32.3, 32.9 (q × 2, J = 125 Hz, CMe_2), 34.2 (t, J = 120 Hz, CH_2), 55.4 (s, CMe_2), 97.3 (s, C_5Me_5), 90.2, 99.4, 99.9, 103.6, 104.9 (s × 5, η^5-$C_5Me_4CH_2$), 131.0 (d, J = 159 Hz, =CH), 215.7, 216.1 (s, Fe-CO), 279.5 (s, μ-CO), 286.7 (s, μ-C=C). IR: (CH_2Cl_2) 1916, 1764 cm^{-1}. FD-MS: m/z 532 (M^+). Anal. Calcd for $C_{28}H_{34}O_3Fe_2$: C, 63.42; H, 6.46. Found: C, 63.41; H, 6.62.

Reaction of 3a with $Ru_3(CO)_{12}$ Giving 18k. A THF solution (15 mL) containing **3a** (116 mg, 0.23 mmol) and $Ru_3(CO)_{12}$ (146 mg, 0.23 mmol) was refluxed for 7 h. After removal

of the volatiles under reduced pressure, the residue was subjected to column chromatography. **18k** (37 mg, 26% yield)-was isolated from the second band eluted with hexanes. **18k**: ^{1}H NMR ($CDCl_3$) δ 1.04, 1.74, 1.81, 1.90, 1.94 (3H × 5, s × 5, C_5Me_5), 1.49, 1.69 (15H × 2, s × 2, Cp*$_2$), 3.04 (1H, dd, J = 8.1 and 14.6 Hz, CH_2), 3.18 (1H, dd, J = 2.8, 14.6 Hz, CH_2), 6.13 (1H, dd, J = 3.0 and 8.3 Hz, =CH). ^{13}C NMR ($CDCl_3$): δ 8.5, 9.9 (q, J = 127 Hz, C_5Me_5), 10.0, 10.2, 11.1, 11.4, 22.3 (q × 5, J = 127 Hz, η^5-C_5Me_5), 40.2 (t, J = 125 Hz, CH_2), 56.7 (s, Me*C*[C(Me)=C(Me)]$_2$), 98.0, 98.2 (s, *C*$_5$Me$_5$), 128.4 (dt, J = 154 and 5 Hz, =CH), 133.5, 134.0, 141.0, 142.0 (s, MeC[*C*(Me)=*C*(Me)]$_2$), 214.4, 214.5 (s × 2, CO), 278.4 (s, μ-CO), 286.5 (s, Fe_2C). FD-MS: m/z 640 (M^+). Anal. Calcd for $C_{36}H_{48}O_3Fe_2$: C, 67.51; H, 7.55. Found: C, 66.99; H, 7.66.

Experimental Procedure for X-ray Crystallography. Suitable single crystals were mounted on glass fibers, and diffraction measurements were made on a Rigaku AFC-5, AFC-5R, and AFC7R automated four-circle diffractometer by using graphite-monochromated Mo Kα radiation (λ = 0.710 59 Å). The unit cells were determined and refined by a least-squares method using 20 independent reflections ($2\theta \simeq 20°$). Data were collected with a $\omega-2\theta$ or ω scan techniques. If $\sigma(F)/F$ was more than 0.1, a scan was repeated up to three times and the results were added to the first scan. Three standard reflections were monitored at every 150 measurements. The data processing was performed on a micro vax II computer (data collection) and an IRIS Indigo computer (structure analysis) by using the teXsan structure solving program system obtained from the Rigaku Corp., Tokyo, Japan. Neutral scattering factors were obtained from the standard source.[22] In the reduction of data, Lorentz and polarization corrections were made. An empirical absorption correction (ψ scan) was made, except for **18e**,**k**. Crystallographic data and the results of refinements are summarized in Table 8.

The structures were solved by a combination of the direct methods and Fourier synthesis (SAPI91 and DIRDIF). Details of the refinement procedures are as follows. Hydrogen atoms unless otherwise stated were fixed at the calculated positions (C−H = 0.95 Å) and were not refined. **3a**: All the non-hydrogen atoms were refined anisotropically, and H1 and H2 were located by examination of Fourier maps and were refined isotropically. **3b**: The *C*-centered monoclinic crystal system was established at first. However, because the *b* axis was too long for a measurement, the data were collected according to a triclinic system (a = 32.74(1) Å, b = 9.631(4) Å, c = 9.594(3) Å, α = 119.91(2)°, β = 81.66(3)°, γ = 94.02(3)°) and then converted to the monoclinic system.[23] In the reduction of the data, the equivalent reflections were averaged. The unit cell contained two independent molecules, and all the non-hydrogen atoms were refined anisotropically. **3c′**: All the non-hydrogen atoms were refined anisotropically. **4**: Because of the limited number of data, the Cp* carbon atoms were refined isotropically and the other non-hydrogen atoms were refined anisotropically. **11c**: During the course of the refinement, it was found that the C2 and C3 atoms were disordered. The occupancy factors of the carbon atoms of the two components (C2a−C2b and C3a−C3b) were determined to be 0.5:0.5. All the non-hydrogen atoms were refined anisotropically. **15b**: Because of the limited number of the data, only Fe, P, C1, C2, C9, C14, O9, and O14 were refined anisotropically and the

Table 8. Crystallographic Data

	3a	**3b**	**3c′**	**4**	**11c**·BF_4·CH_2Cl_2	**15b**	**18e**	**18h**	**18k**	**19**
formula	$C_{26}H_{32}O_3Fe_2$	$C_{28}H_{36}O_3Fe_2$	$C_{36}H_{52}O_3Fe_2$	$C_{35}H_{48}O_5Fe_2$	$C_{33}H_{39}O_3Fe_2BF_4Cl_2$	$C_{42}H_{45}O_2PFe$	$C_{28}H_{38}O_3Fe_2$	$C_{34}H_{36}O_3Fe_2$	$C_{36}H_{48}O_3Fe_2$	$C_{30}H_{30}O_3Fe_2$
fw	504.2	532.3	644.5	660.5	753.1	668.6	534.3	604.3	640.5	550.3
recrystallization solvent	acetone	acetone	ether−hexanes	ether−hexanes	CH_2Cl_2−hexanes	toluene−MeOH	CH_2Cl_2−hexanes	CH_2Cl_2−hexanes	CH_2Cl_2−hexanes	CH_2Cl_2−hexanes
cryst syst	monoclinic	monoclinic	triclinic	orthorhombic	monoclinic	monoclinic	monoclinic	monoclinic	triclinic	monoclinic
space group	$P2_1/n$	Cc	$P\bar{1}$	$Pca2_1$	$P2_1/n$	$P2_1/n$	$P2_1/a$	$P2_1/c$	$P\bar{1}$	$P2_1/c$
a, Å	10.197(3)	9.592(4)	11.339(5)	19.354(7)	14.890(2)	18.473(8)	17.129(8)	9.408(4)	11.059(7)	15.625(5)
b, Å	13.771(2)	64.74(2)	17.631(4)	17.001(6)	16.496(2)	11.165(6)	9.697(3)	17.486(10)	17.385(8)	9.063(3)
c, Å	17.232(5)	9.626(4)	9.355(4)	10.081(6)	15.854(2)	19.126(7)	16.591(7)	18.352(9)	9.240(2)	17.377(4)
α, deg			99.44(3)						94.88(3)	
β, deg	99.15(2)	119.85(3)	112.09(3)		115.160(9)	111.79(3)	104.67(3)	91.33(4)	101.88(4)	93.23(2)
γ, deg			82.93(3)						108.25(4)	
V, Å^3	2388(1)	5185(3)	1705(1)	3317(4)	3524.5(8)	3663(2)	2665(3)	3018(2)	1629(1)	2456(1)
Z	4	8	2	4	4	4	4	4	2	4
d_{calcd}, g·cm^{-3}	1.53	1.36	1.26	1.32	1.42	1.21	1.33	1.33	1.31	1.49
μ, cm^{-1}	12.4	11.4	8.8	9.1	10.3	4.88	11.1	9.9	9.2	12.1
2θ, deg	5−55	5−50	5−50	5−55	5−55	5−45	3−50	5−50	3−50	5−55
diffractometer	AFC5R	AFC5R	AFC5R	AFC5R	AFC7R	AFC5R	AFC5	AFC5R	AFC5	AFC5R
no. of data collected	6027	10376	6317	4199	8706	5265	5151	5857	6108	6228
no of data with $I > 3\sigma(I)$	3121	3847	2905	1884	4986	1632	2747	1326	4138	2856
no. of variables	288	593	370	278	424	225	306	167	382	226
R	0.044	0.044	0.090	0.071	0.060	0.081	0.052	0.099	0.063	0.070
R_w	0.034	0.046	0.085	0.045	0.046	0.055	0.044	0.075	0.057	0.056

(22) *International Tables for X-Ray Crystallography*; Kynoch Press: Birmingham, 1975; Vol. 4.

(23) A reviewer of ref 6 suggested another C-centered monoclinic space group with the cell parameters of a = 16.692(7) Å, b = 9.593(4) Å, c = 33.43(1) Å, β = 103.35(4)°, and V = 5186(3) Å^3. Although the reviewer expected a centric space group, the structure was refined successfully according to an acentric space group (C2). In addition, differences in some structural parameters for the two independent molecules are larger than those reported in this paper. Therefore we adopt the crystal system shown in Table 8, though we also question the very long *b* axis.

other non-hydrogen atoms were refined isotropically. **18e**: All the non-hydrogen atoms were refined anisotropically, and H1 and H2 were located by examination of Fourier maps and were refined isotropically. **18h**: Because of the limited number of the data, only Fe1 and Fe2 were refined anisotropically and the other non-hydrogen atoms were refined isotropically. **18k**: All the non-hydrogen atoms were refined anisotropically, and H2, H3a, and H3b were located by examination of Fourier maps and were refined isotropically. **18l**: All the non-hydrogen atoms were refined anisotropically, and all the hydrogen atoms were located by examination of Fourier maps and were refined isotropically. The occupancy of C2, O2, and H2 was 0.25, 0.25, and 0.5, respectively. **19a**: During the course of the refinement, it was found that the Cp* ring carbon atoms attached to Fe2 were disordered, and they were refined by using two rigid models with independent isotropic thermal parameters for each carbon atom.

Acknowledgment. We are grateful to the Ministry of Education, Science, Sports and Culture of the Japanese Government for financial support of the research. We thank Professor Hiroharu Suzuki and Dr. Masato Oshima of the Tokyo Institute of Technology for collection of the X-ray diffraction data of **11c**.

Supporting Information Available: Tables of positional parameters and B_{eq} values, anisotropic thermal parameters, and bond lengths and angles for **3a**, **3b**, **3c′**, **15b**, **4**, **11c**, **19**, **18e**, **18h**, **18i**, and **18l** and diagrams with atomic numbering scheme for **3b** (molecule 2), the PPh_3 ligand in **15b**, the anionic and solvent part of **11c**, the disordered Cp* part of **19**, and **18l** (54 pages). Ordering information is given on any current masthead page.

OM961104E